โครงสร้างโมเลกุลและสมบัติทางอิเล็กทรอนิกส์ของพอร์ไฟริน-โอลิโกไทโอฟีน- เพอริลีน โดยการคำนวณทางเคมีควอนตัม

นางสาวตติยา โชคบุญเปี่ยม

วิทยานิพนธ์นี้เป็นส่วนหนึ่งของการศึกษาตามหลักสูตรปริญญาวิทยาศาสตรมหาบัณฑิต
สาขาวิชาปิโตรเคมีและวิทยาศาสตร์พอลิเมอร์
คณะวิทยาศาสตร์ จุฬาลงกรณ์มหาวิทยาลัย
ปีการศึกษา 2551

MOLECULAR STRUCTURE AND ELECTRONIC PROPERTIES OF PORPHYRIN-OLIGOTHIOPHENE-PERYLENE USING QUANTUM CHEMICAL CALCULATION

Miss Tatiya Chokbunpiam

A Thesis Submitted in Partial Fulfillment of the Requirements
for the Degree of Master of Science Program in Petrochemistry and Polymer Science
Faculty of Science
Chulalongkorn University
Academic Year 2008

Thesis Title MOLECULAR STRUCTURE AND ELECTRONIC PROPERTIES OF PORPHYRIN-OLIGOTHIOPHENE-PERYLENE USING QUANTUM CHEMICAL CALCULATION
By Miss Tatiya Chokbunpiam
Field of Study Petrochemistry and Polymer Science
Thesis Advisor Professor Supot Hannongbua, Dr.rer.nat.
Thesis Co-Advisor Assistant Professor Patchanita Thamyongkit, Dr.rer.nat.

Accepted by the Faculty of Science, Chulalongkorn University in Partial Fulfillment of the Requirements for the Master 's Degree

…………………………………………… Dean of the Faculty of Science
(Professor Supot Hannongbua, Dr.rer.nat.)

THESIS COMMITTEE

………………………………………………… Chairman
(Assistant Professor Warinthorn Chavasiri, Ph.D.)

………………………………………………… Thesis Advisor
(Professor Supot Hannongbua, Dr.rer.nat.)

………………………………………………… Thesis Co-Advisor
(Assistant Professor Patchanita Thamyongkit, Dr.rer.nat.)

…………………………………………………. Examiner
(Assistant Professor Voravee P. Hoven, Ph.D.)

…………………………………………………. External Examiner
(Arthorn Loisruangsin, Ph.D)

ตติยา โชคบุญเปี่ยม: โครงสร้างโมเลกุลและสมบัติทางอิเล็กทรอนิกส์ของพอร์ไฟริน-โอลิโกไทโอฟีน-เพอริลีนโดยการคำนวณทางเคมีควอนตัม. (MOLECULAR STRUCTURE AND ELECTRONIC PROPERTIES OF PORPHYRIN-OLIGOTHIOPHENE-PERYLENE USING QUANTUM CHEMICAL CALCULATION) อ. ที่ปรึกษาวิทยานิพนธ์หลัก: ศ. ดร. สุพจน์ หารหนองบัว, อ. ที่ปรึกษาวิทยานิพนธ์ร่วม: ผศ. ดร. พัชณิตา ธรรมยงค์กิจ, 76 หน้า.

สารประกอบชนิดใหม่ที่ประกอบด้วยโมเลกุลพอร์ไฟริน (Por) และ เพอริลีน (Per) ที่เชื่อมต่อกันโดยโมเลกุลไทโอฟีนได้ถูกออกแบบและใช้ชื่อย่อว่า Por-Per, Por-Thio-Per, Por-2Thio-Per, และ Por-3Thio-Per โดยการเปลี่ยนแปลงวงไทโอฟีนตั้งแต่ 0 ถึง 3 วง ศึกษาโครงสร้างและสมบัติทางอิเล็กทรอนิกส์ของสารประกอบเหล่านี้ โดยใช้ระเบียบวิธีทางเคมีควอนตัม ซึ่งจากข้อมูลพบว่า วิธี B3LYP/6-31G(d) เป็นวิธีหนึ่งที่มีความเหมาะสมเมื่อพิจารณาทั้งในแง่ของความถูกต้องและเวลาที่ใช้ในการคำนวณ ทั้งนี้โครงสร้างเสถียรของ Por-Thio-Per ได้ถูกนำมาศึกษาผลของหมู่แทนที่แบบ mono และ bi ที่ถูกแทนที่ที่ตำแหน่ง R บนคาร์บอนอะตอมตำแหน่งที่ 3 และ R′ บนคาร์บอนอะตอมตำแหน่งที่ 4 ของวงไทโอฟีน ผลการศึกษาชี้ให้เห็นว่ามีผลต่อการเปลี่ยนแปลงมุมของการบิดระหว่างระนาบของวงพอร์ไฟรินและวงเพอริลีนอย่างมีนัยสำคัญสำหรับการเติมหมู่แทนที่แบบ bi จำนวน 2 หมู่แทนที่ได้แก่ $-OCH_3$ และ $-NH_2$ และแบบ mono จำนวน 1 หมู่แทนที่โดยที่ R= –H และ R′ = $-NH_2$ ซึ่งผลสรุปที่น่าสนใจคือการลดลงของค่าช่องว่างแถบอิเล็กตรอนระหว่าง HOMO-LUMO จะพบเฉพาะกรณีของการเติมหมู่แทนที่ชนิดให้อิเล็กตรอนแบบ mono เท่านั้น และพบการเปลี่ยนแปลงของค่าช่องว่างแถบอิเล็กตรอนในการเพิ่มจำนวนวงไทโอฟีนอีกด้วย นอกจากนี้ยังพบว่าการดูดกลืนแสงในช่วงคลื่นยูวี-วิสิเบิลของสารประกอบทั้งหมดที่ศึกษาอยู่ครอบคลุมในช่วงที่กว้างขึ้นในช่วง 370-730 nm โดยที่สมบัติการดูดกลืนแสงของโมเลกุลพอร์ไฟรินและเพอร์ริลีนยังคงอยู่ ในช่วง 372 และ 473 nm ตามลำดับ

สาขาวิชา...ปิโตรเคมีและวิทยาศาสตร์พอลิเมอร์ ลายมือชื่อนิสิต..
ปีการศึกษา…2551…………………………… ลายมือชื่อ อ. ที่ปรึกษาวิทยานิพนธ์หลัก...........
ลายมือชื่อ อ. ที่ปรึกษาวิทยานิพนธ์ร่วม...........

5072275532: PETROCHEMISTRY AND POLYMER SCIENCE
KEYWORDS: ORGANIC DYE-SENSITIZED SOLAR CELL / PORPHYRIN / PERYLENE / THIOPHENE / QUANTUM CALCULATION.

TATIYA CHOKBUNPIAM: MOLECULAR STRUCTURE AND ELECTRONIC PROPERTIES OF PORPHYRIN-OLIGOTHIOPHENE-PERYLENE USING QUANTUM CHEMICAL CALCULATION. THESIS ADVISOR: PROF. SUPOT HANNONGBUA, Dr. rer. nat., THESIS CO-ADVISOR: ASST. PROF. PATCHANITA THAMYONGKIT, Dr. rer. nat., 76 pp.

A new series of compounds consisting of porphyrin (Por) molecule linked to perylene (Per) unit via a thiophenic bridge are designed, namely, Por-Per, Por-Thio-Per, Por-2Thio-Per, and Por-3Thio-Per by varying the number of thiophene ring from 0 to 3, respectively. Structural and electronic properties of those compounds were studied using quantum calculation approach. The method used was validated and found that the B3LYP/6-31G(d) is the optimal one compromising between the accuracy and the computer time required. With optimal structure of Por-Thio-Per, the effect of mono- and bi-substituents R on C3 and R′ on C4 of thiophene ring was studied. It was shown that significant changes of the torsion angle between the molecular planes of the Por and Per rings were found only for the two bi-substituted derivatives, R = R′ = $-OCH_3$ and $-NH_2$, and one mono-substituted derivative, R = –H and R′ = $-NH_2$. Noticeable decreases of the HOMO-LUMO energy gap were found only when the mono-substituents are the electron donor groups. In addition, The significant change of the HOMO-LUMO energy gap was also observed as the function of number of thiophene ring. The UV-visible spectra of all proposed compounds cover a broader range, 370-730 nm and characteristics of the Por and Per molecules, which indicate by the absorptions spectra at 372 and 473 nm, remain unchanged.

Field of study:…Petrochemistry and Polymer science Student’s signature:…………...
Academic year: ……2008…… Advisor’s signature:………….
Co-Advisor’s signature:……….

ACKNOWLEDGEMENTS

This work would not be possible without who support and encourage. I would like to clarify that throughout the work a number of people have cooperated in many different ways.

First of all, I would like to gratefully thank my advisor Prof. Dr.rer.nat. Supot Hannongbua and co-advisor Asst. Prof. Dr.rer.nat. Patchanita Thamyongkit for all advices and helps. I also would like to thank Assoc. Prof. Dr. Vudhichai Parasuk, Dr. Piti Treesukol, and Dr. Oraphan Saengsawang for several nice suggestions, discussion and cheer me up in hard time.

I would like to thank Asst. Prof. Dr. Warinthorn Chavasiri, Assoc. Prof. Dr. Sirirat Kokpol, Asst. Prof. Dr. Voravee P. Hoven, Dr. Tawun Remsungnen, and Dr. Arthorn Loisruangsin who act as the thesis committee.

Special thanks go to my friends and family, who supported me throughout this project. Their unconditional love is the source of my strength.

Finally, I also would like to acknowledge the Thailand Research Fund-Master Research Grants-Window II (TRF-MRG-WII Project 515S045) collaboration with Chulalongkorn university and National Center of Excellence for Petroleum, Petrochemicals, and Advanced Materials are gratefully acknowledged for financial supporting. All facilities and computer resources are provided by the Computational Chemistry Unit Cell (CCUC) at Department of Chemistry, Faculty of Science, Chulalongkorn University.

CONTENTS

LIST OF TABLES

Table **Page**

LIST OF FIGURES

LIST OF ABBREVIATIONS

Å = Angstrom

B3LYP = Beck’s three parameter hybrid functional using the LYP correlation function

DFT = Density functional theory

eV = Electron volt

HOMO = Highest occupied molecular orbital

HF = Hatree-Fock

kcal/mol = Kilocalorie per mole

KS = Kohn-Sham

LUMO = Lowest unoccupied molecular orbital

LYP = Lee-Yang-Parr functional

MO = Molecular orbital

N = Number

Per = Perylene molecule

Por = Porohyrin molecule

Por-Per = Porohyrin-Perylene compound

Por-Thio-Per = Porohyrin-Thiophene-Perylene compound

Por-2Thio-Per = Porohyrin-2Thiophene-Perylene compound

Por-3Thio-Per = Porohyrin-3Thiophene-Perylene compound

QM = Quantum mechanics

STO = Slater type orbital

STO-3G = Slater type orbital approximated by 3 gaussian type orbitals

TD-DFT = Time-dependent density functional theory

Thio = Thiophene molecule

CHAPTER I

INTRODUCTION

1.1 Research rationale.

Since the present cost of electricity from silicon-based photovoltaics (PVs) is much higher than the current commercial prices of electricity generated by hydraulic power, nuclear and fossil fuels. Therefore, it is necessary to develop low-cost solar cells with high power conversion efficiency [1-5]. As promising candidates to fulfill these requirements, organic-based solar cells have attracted attention of scientists. One of the key developments of organic compounds for dye-sensitized solar cells comes from the molecular design in order to tune photophysical, electrochemical and optical properties of the molecules [6-11]. This becomes the main propose of this study which focus to design a new series of compounds consisting of porphyrin macrocycle linked to perylene unit via a thiophenic bridge that exhibiting an extended absorption range, narrow band gap and potential electronic transfer by using quantum chemical calculation.

1.2 Solar cell.

1.2.1 What is a solar cell?

A solar cell or photovoltaic cell is a device which generates electricity directly from visible light by means of the photovoltaic effect. In order to generate useful power, it is necessary to connect a number of cells together to form a solar panel, also known as a photovoltaic module. There is more about the different types of solar cell The nominal output voltage of a solar panel is usually 12 Volts, and they may be used singly or wired together into an array. The number and size required is determined by the available light and the amount of energy required.

1.2.2 Types of solar cells.

Commercial solar cells are usually made from silicon, the same material used for transistors and integrated circuits. The silicon is treated or "doped" so that when light strikes it electrons are released, so generating an electric current. There are three basic types of solar cell [12,13].

- Monocrystalline silicon

This type of solar cell uses a single layer of silicon for the semi-conductor. In order to produce this type of silicon, it must be extremely pure which means it is the most expensive type of solar cell to produce.

- Polycrystalline silicon

To make polycrystalline silicon cells, liquid silicon is poured into blocks that are subsequently sawed into plates. This type of approach produces some degree of degradation of the silicon crystals which makes them less efficient. However, this type of approach is easier and cheaper to manufacture.

- Amorphous thin film silicon

This type of solar cell uses layers of semiconductor that are only a few micrometers thick (about 1/100th the thickness of a human hair). This lowers the material cost but makes it even less efficient than the other types of silicon. However, because it is so thin this type of cell has the advantage that it can be placed on a wide variety of flexible materials in order to make things like solar shingles or roof tiles.

Another way of looking at solar cells is in terms of the types of materials they are made with. While silicon is the most commonly used crystal, a number of other materials can be used as well. These include the following: gallium arsenide (GaAs), copper indium diselenide (CIGS), and cadmium telluride (CdTe) [14].

1.2.3 Generations of solar cells [15].

- First generation solar cells

These cells are the larger, silicon-based photovoltaic cells that have, still, dominate the solar panel market due to their high efficiency. These solar cells, using silicon wafers, account for 86% of the solar cell market. This despite their high manufacturing costs; a problem that second generation cells hope to remedy.

- Second generation solar cells

To simplify manufacturing and reduce costs, a second generation known as thin film technologies was developed. These technologies are typically made by depositing a thin layer of a photo-active material onto glass or a flexible substrate, including metal foils. They commonly use amorphous silicon, CIGS, and CdTe as the semiconductor. Thin film PV is less subject to breakage when manufactured on a flexible foil. However, the promise of low cost power has not been realized, and efficiency remains lower than that of the first generation solar cell.

- Third generation solar cells

It has been estimated that 3rd generation solar technologies will achieve higher efficiencies and lower costs than the first or second generation technologies**.** Today, the 3rd generation approaches being investigated include dye-sensitized solar cells and organic solar cells.

1.3 Dye-sensitized solar cell [16].

Dye-sensitized solar cell (DSSC) is a real revolution in solar energy after 40 years of the invention of silicon solar cell. The working mechanism is based on photoelectrochemical mechanism, resembling the photosynthesis in plant leaves. This cell was invented by Michael Grätzel and are also known as Grätzel cells as shown in Figure 1.1.

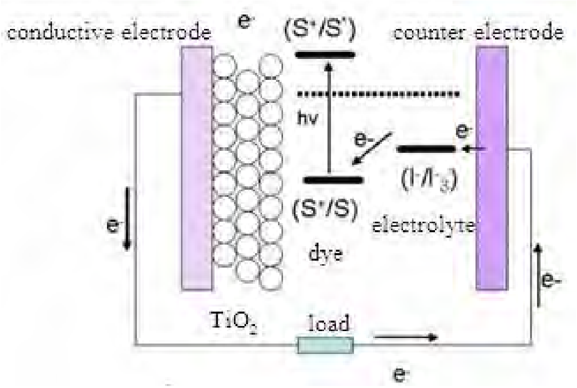

Figure 1.1. Operation principle of a dye-sensitized solar cell.

As the dye molecules are hit by light, electrons in the dye are transmitted to TiO_2. Then the electrons are collected by conductive electrode and supplied to external load. The dye molecules are then electrically reduced to their initial states by electrons transferred from redox couple in the electrolyte. The oxidized ions in the electrolyte diffuse to the counter electrode to receive electrons. The redox reactions occurring in the electrolyte are:

$$\text{Oxidation:} \quad 3I^- \rightarrow I^-_3 + 2e^-$$

$$\text{Reduction:} \quad I^-_3 + 2e^- \rightarrow 3I^-$$

1.4 Organic dye molecules.

The key to the development of organic dye solar cells is considered to be the design and organization of organic compounds (π-conjugated organic materials). In addition to tuning of the optical/electrochemical physical properties and functions of molecules and among molecules, the development of crystalline materials, which display high electron and hole mobility, is desirable, regardless of whether the material is a p-type or an n-type organic semiconductor.

1.4.1 Porphyrin.

Porphyrins are a ubiquitous class of naturally occurring compounds with many important biological representatives including hemes, chlorophylls, and several others. All of these molecules share in common the porphyrin macrocyclic substructure. The basic structure of the porphyrin macrocycle consists of four pyrrolic subunits linked by four methine bridges as shown in Figure 1.2a. Porphyrins are aromatic and they obey Huckel's rule for aromaticity in that they posess 4n+2 pi electrons which are delocalized over the macrocycle. Porphyrin and their derivatives are highly colored absorbing strongly in the visible region near 400 nm characteristic of the macrocyclic conjugation and several weaker absorption bands between 450-700 nm. Importantly, they have a donor or p-type character, including energy-transfer and charge carrier [17-19].

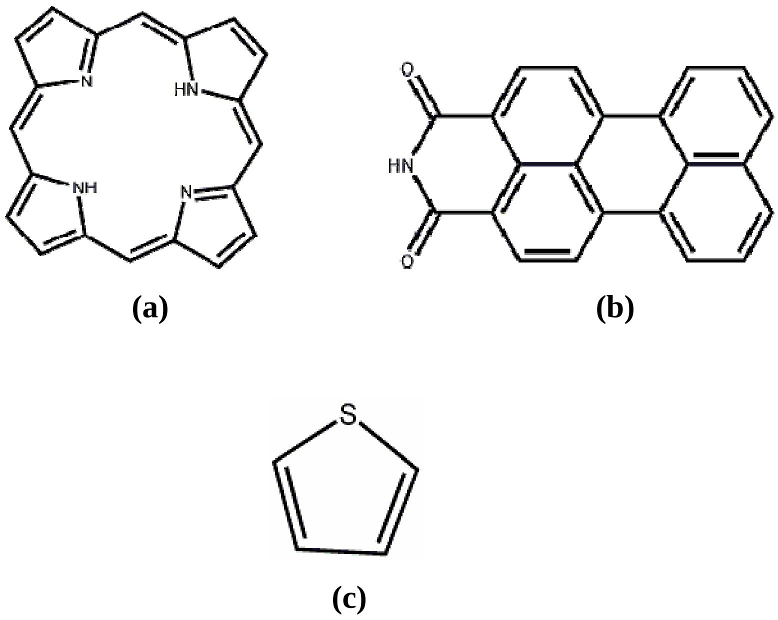

(a) (b)

(c)

Figure 1.2. Chemical structures of (a) free base porphyrin, (b) perylene, and (c) thiophene molecules.

1.4.2 Perylene.

Perylene is a polycyclic aromatic hydrocarbon by it consists of two naphthalene molecules connected by a carbon-carbon bond at the 1 and 8 positions on both molecules as shown in Figure 1.2b. Perylene dyes and its derivatives are excellent acceptor or n-type molecules and exhibit strong light absorption in a range of 450-550 nm, with a sizable electron mobility [20].

1.4.3 Thiophene.

Thiophene, also known as thiofuran, is a heterocyclic compound with the formula C_4H_4S as shown in Figure 1.2c. Thiophene is an analog to furan and pyrrole where the sulfur atom is replaced by O and NH, respectively. It is the simplest aromatic compound containing sulfur atom and it shares some similar chemical properties with benzene. The lone electron pairs on sulfur in the delocalized pi-electron system does not exhibits the properties of thioethers but aromaticity. The polymer formed by linking thiophene through its 2,5 positions is called polythiophene. More useful are polymers derived from thiophenes substituted at the

3-position or 3- and 4- positions. Moreover, in solar cell application, pi-conjugated system becomes a bridge in transportation of charges between p-type and n-type organic semiconductor [21,22].

1.5 Literature reviews.

DSSC have been attracted interest of scientists from many fields. With the variously modified structures and non toxic environment applications, DSSC was supposed to be new promising energy sources. The π-conjugated system in organic dye compound can absorb light and transform it to energy via electron transfer. A lot of experiments and researches are performed to investigate the use of organic dyes such as porphyrin, perylene, and thiophene for increase light absorption and efficiency in solar cells.

In 2000, Baffreau *et al.*[23] reported electronic structures of complex molecular systems containing fullerene C_{60} covalently linked to perylenediimide (PDI) using ab initio Density Functional Theory (DFT) and Hartree–Fock (HF) methods. Semi-empirical PM3 calculations have been used to obtain the optimized geometries, giving an excellent correlation between the torsion angles of the PDI core tetrasubstituted on the bay region and the crystallographic values. A satisfactory agreement was found using the DFT/B3LYP method (basis 6-31G(d,p)), between the theoretically calculated LUMO energies and the cathodic peak potentials measured by cyclic voltammetry of perylenediimide-C_{60} dyads.

In 2000, Sundholm *et al.*[8] investigated electronic absorption spectrum of free-base porphyrin at density functional theory (DFT) level using the time-dependent perturbation theory approach. The optimization of the molecular structure was carried out using the Becke-Perdew function. The calculated absorption spectrum was in agreement with recently ab initio and DFT calculations and also with experiment. The lowest symmetry-allowed triplet-triplet transition was calculated to be 1.58 eV as compared to the experimental value of 1.56–1.58 eV.

In 2003, Hara *et* al.[24] have developed new coumarin dyes having thiophene moieties in order to investigate the photovoltaic performance of dye-sensitized nanocrystalline TiO_2 solar cells based on the organic dyes as photosensitizers. A solar-energy-to-electricity conversion efficiency of 7.7% was attained under AM 1.5 irradiation.

In 2006, De *et al*. [25] studied the bichromophores comprising a donor molecule 4-methoxy-benzo[b]thiophene (4MBT) and an acceptor molecule *p*-chloro-acetophenone (PCA) linked together by unsaturated or saturated olefinic spacers, –CH═CH– and $–CH_2–CH_2$. The difference between the ground and excited singlet state dipole moments confirmed the electron transfer probability. The possibility of formation of ground state charge transfer complex in case of the bichromophoric systems is indicated by time dependent density functional theory (TD-DFT) with B3LYP/6-311G(d,p) theoretical and semi-empirical RHF-SCF-PM3 calculation and confirmed experimentally by electronic absorption (UV–Vis) spectroscopic measurements.

In 2006, Muhlbacher *et al.*[26] reported the results of bulk heterojunction polymer solar cells with this low-band gap polymer showing the highest photocurrent response so far for this class of materials. Efficiencies up to 3.2% were realized when poly[2,6-(4,4-bis-(2-ethylhexyl)-4H-cyclopenta[2,1-b;3,4-b']-dithiophene)-alt-4,7(2,1,3-benzothiadiazole)] (PCPDTBT) blended with phenyl C_{71} butyric acid methyl ester (PC71BM). These conjugated polymer have the intrinsic capability to reach provide a 7% efficiency.

In 2007, Choi *et al.*[10] designed and synthesized the novel organic dyes containing [bis(9,9-dimethylfluoren-2-yl)amino]benzo[b]thiophene as electron donor and cyano acrylic acid as electron acceptor bridged by a thiophene or vinylene thiophene unit. They reported two new organic dyes conversion efficiency of 7.43% and 5.49%.

In 2007, Kim *et al.*[11] designed and synthesized the novel unsymmertrical organic sensitizers consisting of a bis-dimethylfluoreneaniline moiety acting as electron donor and cyano acrylic acid as electron acceptor, connected by thiophene-ethylene unit. They also investigated the effect of methyl or hexyl on thiophene bridge by B3LYP/3-21G(d) calculations. Under standard global AM 1.5 solar condition, thiophene-ethylene bridge gave high efficiency.

In 2007, Nilsing *et al.*[27] studied the absorbtion of perylene derivatives on the rutile TiO_2 (110) surface by quantum-chemical periodic calculations employing the hybrid HF-DFT functional B3LYP. The perylene molecule was functionalized by attachment of phosphonic acid or carboxylic groups to permit anchoring to the metal oxide surface. The phosphonic acid anchoring group was found to bind the perylene derivatives much more strongly to the surface than carboxylic acid anchoring group.

Numerous experimental methods have been applied to acquire novel organic dyes with higher efficiency. Although experimental molecular modification is a powerful and straightforward route to get new dyes, the synthesis process is not only expensive but time-consuming. Theoretical calculation method is another powerful tool for molecular design, and conclusion drawn from calculation are valuable guideline for synthesis of new efficient dyes. The main propose of the research is to design new compound consisting of porphyrin macrocycle linked to perylene unit via a thiophenic bridge that may exhibit an extended absorption range and electronic transfer by using quantum chemical calculation.

1.6 Scope of this study.

This study includes the structural investigation in terms of conformational search, and the determination of electronic properties, in terms of highest occupied molecular orbital (HOMO), lowest unoccupied molecular orbital (LUMO), band gap energies as well as absorption spectra of the Porphyrin-Perylene (Por-Per), Porphyrin-Thiophene-Perylene (Por-Thio-Per), Porphyrin-2Thiophene-Perylene (Por-2Thio-Per), and Porphyrin-3Thiophene-Perylene (Por-3Thio-Per) compounds using quantum chemical calculation. In addition, excitation states and frontier molecular orbitals of the compounds were also analyzed.

CHAPTER II

THEORY BACKGROUND

Nature itself on a micro or macroscopic scale can be described by equations with computational algorithms. The thing with matter in nature is that it may behave as particle and as waves at the same time. The phenomenon is crucial when describing processes at the molecules, atoms and electrons level. This is the case when dealing with processes and properties in a photo electrochemical system as the DSSC. An accurate description of these systems requires quantum chemistry, quantum mechanics, and the central equation is the Schrödinger equation [28].

2.1 Quantum chemistry [29].

Computational chemistry has become a useful way to investigate materials that are too difficult to find or too expensive to purchase. It also helps chemists make predictions before running the actual experiments so that they can be better prepared for making observations. The Schroedinger equation is the basis for most of the computational chemistry scientists use. This is because the Schroedinger equation models the atoms and molecules with mathematics. For instance, you can calculate:

- Electronic structure determinations
- Geometry optimizations
- Frequency calculations
- Transition structures
- Protein calculations, i.e. docking
- Electron and charge distributions
- Potential energy surfaces
- Rate constants for chemical reactions
- Thermodynamic calculations- heat of reactions, energy of activation

Quantum chemistry mathematically describes the fundamental behavior of matter at the molecular scale. It is, in principle, possible to describe all chemical systems using this theory. In practice, only the simplest chemical systems may realistically be investigated in purely quantum mechanical terms, and approximations must be made for most practical purposes (e.g., Hartree-Fock, post Hartree-Fock or Density functional theory, see computational chemistry for more details). Hence a detailed understanding of quantum mechanics is not necessary for most chemistry, as the important implications of the theory (principally the orbital approximation) can be understood and applied in simpler terms.

In quantum mechanics the Hamiltonian, or the physical state, of a particle can be expressed as the sum of two operators, one corresponding to kinetic energy and the other to potential energy. The Hamiltonian in the Schrödinger wave equation used in quantum chemistry does not contain terms for the spin of the electron.

2.2 Quantum mechanics [30].

Quantum mechanics (QM) is a branch of physics dealing with the behavior of matter and energy on the minute scale of atoms and subatomic particles. Quantum mechanics is fundamental to our understanding of all of the fundamental forces of nature except gravity.

Quantum mechanics is the foundation of several branches of physics, including electromagnetism, particle physics, condensed matter physics, and even parts of cosmology. Quantum mechanics is also essential to the theory of chemical bonding (and hence all of chemistry), structural biology, and technologies such as electronics, information technology, and nanotechnology. A century of experiments and of work in applied science has proved quantum mechanics successful and practical.

Quantum mechanics began in the early 20th century, with the pathbreaking work of Max Planck and Niels Bohr. Max Born coined the term "quantum mechanics" in 1924. The wider physics community soon accepted quantum mechanics because of its highly accurate empirical predictions, especially in systems where Newtonian mechanics fails. A major early success of quantum mechanics was its explanation of wave-particle duality, namely of how subatomic particles have wave-like properties and waves have particle-like properties. Quantum mechanics also applies to a wider range of situations than general relativity does, e.g., to systems whose scale is atomic or smaller, and to those having very low or very high energies or subjected to the lowest temperatures.

2.3 Schrödinger equation [28, 31].

In physics, especially quantum mechanics, the Schrödinger equation is an equation that describes how the quantum state of a physical system changes in time. It is as central to quantum mechanics as Newton's laws are to classical mechanics. In the standard interpretation of quantum mechanics, the quantum state, also called a wavefunction or state vector, is the most complete description that can be given to a physical system. Solutions to Schrödinger's equation describe atomic and subatomic systems, electrons and atoms, but also macroscopic systems, possibly even the whole universe. Schrödinger's equation can be mathematically transformed into Heisenberg's matrix mechanics, and into Feynman's path integral formulation. The Schrödinger equation describes time in a way that is inconvenient for relativistic theories, a problem which is not as severe in Heisenberg's formulation and completely absent in the path integral.

The systems in quantum chemistry refer to atoms and molecules, which consist of a number of nuclei and electrons. The total energy for this kind of system has five contributions: kinetic energies of each nuclei and electron (T_e and T_n), attraction between each electron and nuclei (V_{en}), internuclear and interelectronic repulsion potential energy (V_{ee} and V_{nn}).

2.4 Born-Oppenheimer approximation [32].

In order to be able to solve Schrödinger's equation for any system larger than an atom with one electron, various approximations need to be made. Each of these approximations contributes its own inaccuracies to the final result, which must be accounted for in reporting results. One of the more important approximations used is the Born-Oppenheimer approximation.

The Born-Oppenheimer approximation is the first of several approximations made when trying to solve Schrödinger's equation for more complex systems than one or two electrons. It is the assumption that the electronic motion and the nuclear motion in molecules can be separated. It leads to a molecular wave function in terms of electron positions and nuclear positions. It separates electron and nuclear motion based on the idea that nuclear mass is so much larger than electron mass that the nuclei are basically "fixed" particles. In this case, since the nuclei are so much more massive than the electrons, they must accordingly have much smaller velocities. Thus it is plausible that on the typical time-scale of the nuclear motion, the electrons will very rapidly relax to the instantaneous ground-state configuration, so that in solving the time-independent Schrödinger equation resulting from the Hamiltonian in equation, we can assume that the nuclei are stationary and solve for the electronic ground-state first, and then calculate the energy of the system in that configuration and solve for the nuclear motion. This separation of electronic and nuclear motion is known as the Born-Oppenheimer approximation.

2.5 Hartree-Fock method [29, 33].

The original Hartree method expresses the total wavefunction of the system as a product of one-electron orbitals. In the Hartree-Fock method, the wavefunction is an antisymmetrized determinantal product of one-electron orbitals (the "Slater" determinant). Schrödinger's equation is transformed into a set of Hartree-Fock equations. The Hartree-Fock approximation is also known at the self-consistent field (SCF) method.

Hartree Fock method is one the simplest approximate theories of the ground-state wavefunction and ground-state energy of a quantum many-body system. Hartree-Fock theory, by assuming a single-determinant from for the wavefunction, neglects correlation between electrons. The electrons are subject to an average non-local potential arising from the other electrons. Therefore, it is a theory that is an approximation of the reality but solved exactly which gives the exact exchange energy but leads to computing four-index integrals. The correlation energy is neglected.

2.6 Density functional theory.

The Density Functional Theory (DFT) is a computationally efficient way of including electron correlation [34]. The system is described by an electron density, rather than a sum of independent electrons, and the Hamiltonian is then only dependent on position and atomic number of the nuclei and the total number of electrons. The governing equation is still the electronic Schrödinger equation but the total energy of the system is expressed as a function of the electron density

DFT is an exact theory and the only approximation is due to that exchange correlation energy is unknown. The basis sets for these Kohn-Sham (KS)-orbitals have fewer requirements than those in Hartree-Fock. They are not needed for calculating exchange and Coulomb interaction which are the most work consuming part of the Hartree-Fock method. This, and the fact that DFT account for electron correlation, make DFT very useful for larger systems. However, the crucial task in DFT is to find an accurate exchange correlation functional. The most popular exchange-correlation functional is the B3LYP functional [35,36]. It consists of several functionals, including the HF exact exchange energy in a three-parametric scheme.

2.7 Basis set.

The set of mathematical functions that constructs the molecular orbital (MO) in the linear combination of atomic orbitals (LCAO) is called a basis set, which is expanded as a linear combination of such functions with weights or coefficients to be determined. Usually these functions are atomic orbitals, in that they are centered on atoms, but functions centered in bonds or lone pairs, and pairs of functions centered in the two lobes of a p orbital, have been used. Additionally, basis sets compose of sets of plane waves down to a cutoff wavelength are often used, especially in calculations involving systems with periodic boundary conditions [33, 37].

2.7.1 Single-ζ, Multiple-ζ, and Split-Valence.

The STO-3G basis set is what is known as a “single- ζ” basis set, or, more commonly, a “minimal” basis set. This nomenclature implies that there is one and only one basis function defined for each type of orbital core through valence. Thus for H and He, there is only a 1s function. For Li to Ne, there are five functions, 1s, 2s, 2p, 2p , and 2p. For Na to Ar, 3s, $3p_x$, $3p_{y,}$ $3\ p_z$ are added to the second-row set, making a total of nine functions, etc. Because the minimal basis set is so small, it is so small, it is not recommended for consistent and accurate predictions of molecular energies.

However, their simple structure provides a good tool for visualizing qualitative aspects of chemical bonding.

One way to increase the flexibility of a basis set is to “decontract” it. That is, we might imagine taking the STO-3G basis set, and instead of constructing each basis function as a sum of three Gaussians, we could construct two basis functions for each AO, the first being a contraction of the first two primitive Gaussians, while the second would simply be the normalized third primitive. This prescription would not double the size of our basis set, since we would have all the same individual integrals to evaluate as previously, but the size of our secular equation would be increased. A basis set with two functions for each AO is called a “double-ζ” basis. Of course, we could decontract further, and treat each primitive as a full-fledged basis function, in which case we would have a‘triple-ζ’ basis, and we could then decide to add more functions indefinitely creating higher and higher multiple- ζ basis sets.

The reason for this is that core orbitals are only weakly affected by chemical bonding. Valence orbitals, on the other hand, can vary widely as a function of chemical bonding. Atoms bonded to significantly more electronegative elements take on partial positive charge from loss of valence electrons, and thus their remaining density is distributed more compactly. The reverse is true when the bonding is a more electropositive element. From a chemical standpoint, then, there is more to be gained by having flexibility in the valence basis functions than in the core, and recognition of this phenomenon led to the development of so-called “split-valence” or “valence-multiple-ζ” basis sets. The core orbitals are represented by minimal basis set whereas the valence shell orbitals are represented by more than one basis function such as 3-21G, 6-21G, 4-31G, 6-31G, and 6-31G, which have one contracted that is a linear combination of three primitive Gaussian for each inner-shell atomic orbital and two basis function, one contracted Gaussian function that is a linear combination of two primitive Gaussian function, for each valence orbital. If there is valence-triple- ζ, like 6-311G, use there sizes of contracted functions for each orbital-type.

2.7.2 Polarization function.

Polarized basis sets allow some small contributions from the unfilled orbital, which is required for the ground state for atomic description by adding orbitals with angular momentum beyond. Pople and co-workers introduced a simple nomenclature scheme to indicate the presence of these functions, the “*” (star). Thus, 6-31G* implies a set of d functions added to polarize the p functions in 6-31G. A second star ** implies p functions on H and He, e.g., 6-31G**. To use more than one set of polarization functions in modern calculation, the standard nomenclature for the Pople basis sets now typically includes an explicit enumeration of those functions instead of the star nomenclature.

2.7.3 Diffuse function.

When a basis set does not have the flexibility necessary to allow a weakly bound electron to localize far from the remaining density (such as molecular with lone pairs, anions and other systems with significant negative charge, systems in their excited states, and system with low ionization potentials), significant errors in energies and other molecular properties can occur. In the Pople family of basis sets, the presence of diffuse function is indicated by a “+”in the basis set name. The 6-31+G(d) indicates that heavy atoms have been augmented with an additional one s and one set of p functions having small exponents.

2.8 Excited state.

An excited state is a state where at least one electron is in a higher energy level compared to the ground state. Information and conclusions of excited states can be drawn by examining the occupied and virtual states in the standard DFT and HF ground state calculations, where the energy differences between the occupied and unoccupied levels resemble the excitation energies. To get more reliable information about the excited states one has to go beyond HF and DFT.

Time-dependent DFT (TD-DFT) is an extension of DFT that handles electronic excited states. Physical properties such as absorption spectra can easily be calculated. For the extraction of the excited states, the system is simply subjected to an external time-dependent electric field that is treated as a small perturbation within a linear response theory. The perturbation can, for instance, be atomic motions or light.

Excitation energies can then be calculated without computing all the excited-state wavefunctions, they are simply determined by poles of the response function. In a variational form, each excitation energy and associated oscillator strength (transition probability) can then be calculated iteratively. For instance, the molecule interaction with light can be modeled by the interaction with an electric field with frequency [38].

TD-DFT gives a good first estimation of physical processes such as photoexcitation, for which information about the excited states is wanted. However, since the virtual orbitals in general are quite poor, this method should be handled with care and only be used for the lowest excitations. For a deeper understanding of TD-DFT, readers are referred to refs [39] and [40].

2.9 Gaussian program [41].

GAUSSIAN is a computational chemistry software program, first written by John Pople. Gaussian's copyright was originally held by Carnegie Mellon University, and later by Gaussian, Inc. Gaussian quickly became a popular and widely-used electronic structure program. Prof. Pople and his research group were among those who pushed the development of the package, including cutting-edge research in quantum chemistry and other fields. Gaussian functions arise by applying the exponential function to a general quadratic function. The Gaussian functions are thus those functions whose logarithm is a quadratic function. The Gaussian functions appear in many contexts in the natural sciences, the social sciences, mathematics, and engineering. Some examples include:

- A Gaussian function is the wave function of the ground state of the quantum harmonic oscillator.
- Gaussian beams are used in optical and microwave systems.
- The molecular orbitals used in computational chemistry can be linear combinations of Gaussian functions called Gaussian orbitals.
- Mathematically, the derivatives of the Gaussian function are used to define Hermite polynomials.

CHAPTER III

CALCULATION DETAILS

3.1 Optimal structure.

The initial structures of the Por-Per, Por-Thio-Per, Por-2Thio-Per and Por-3Thio-Per compounds were generated using GaussView program. As it is successfully used in the previous studies [42-49], the density functional theory (DFT) approach at the B3LYP with the 6-31G(d) basis set was used in this study to search for the optimal structure of the investigated compounds.

3.1.1 Optimal structure of Por-Per compound.

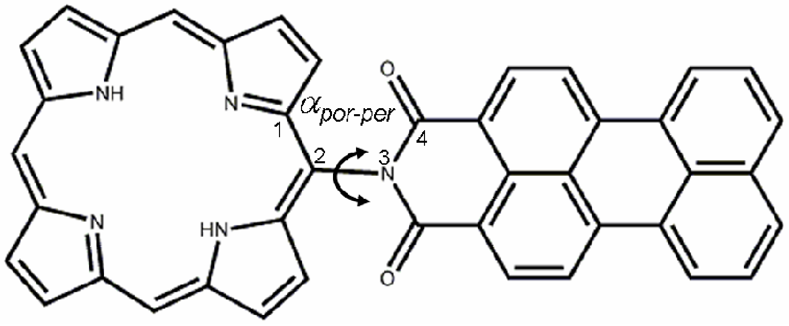

Figure 3.1. Two-dimensional structure of the Por-Per compound where the torsion angle, $\alpha_{por\text{-}per}$, defined by 1-2-3-4.

Here, two procedures were separately applied, (*i*) the structure was fully optimized, *i.e.,* all atoms were allowed to relax. (*ii*) to examine whether the obtained structure is the global minimum energy conformation, torsion angles, $\alpha_{por\text{-}per}$, shown in Figure 3.1 was defined. Then, its geometries, bond lengths and bond angles obtained from (*i*), were kept constant throughout, whereas, the torsion angle was optimized using the following manner. The angle $\alpha_{por\text{-}per}$ was set at 0°. Then, the $\alpha_{por\text{-}per}$ angle was scanned from 0° to 180° with the interval 30°. In order to get more precise conformation, the procedures *(ii)* was, again, repeated in the range around the optimal $\alpha_{por\text{-}per}$ angle with the intervals 5^{o} and 1^{o}.

3.1.2 Optimal structure of Por-Thio-Per compound.

Here, two procedures were separately applied, (*i*) the structure was fully optimized, *i.e.*, all atoms were allowed to relax. (*ii*) to examine whether the obtained structure is the global minimum energy conformation, two torsion angles, $\alpha_{por\text{-}thio}$ and $\alpha_{per\text{-}thio}$, shown in Figure 3.2 were defined. Then, its geometries, bond lengths and bond angles obtained from (*i*), were kept constant throughout, whereas, the torsion angles were optimized using the following manner. The angle $\alpha_{por\text{-}thio}$ was fixed at 0˚ while $\alpha_{per\text{-}thio}$ was scanned from 0˚ to 180˚ with the interval of 30˚. This procedure was, then, repeated by keeping $\alpha_{por\text{-}thio}$ at 30˚, 60˚, 90˚, 120˚, 150˚ and 180˚. In order to get more precise conformation, the procedures *(ii)* was, again, repeated in the range around the optimal $\alpha_{por\text{-}thio}$ and $\alpha_{per\text{-}thio}$ angles with the intervals 5^o and 2^o.

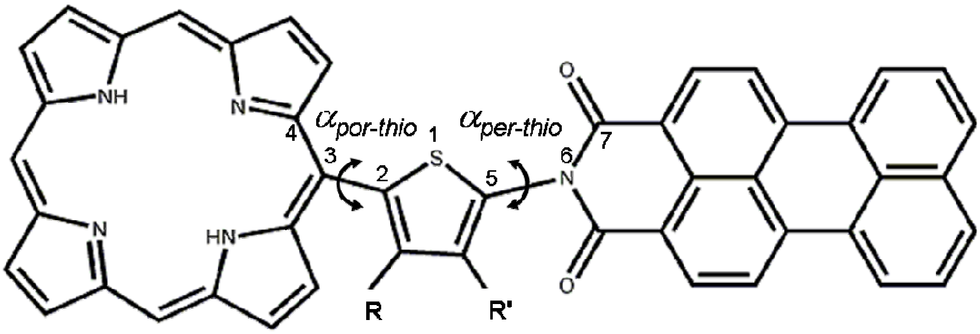

Figure 3.2. Two-dimensional structure of the Por-Thio-Per compound (R = –H, R′ = –H) and its derivatives where (*i*) R = –H, R′ = –H, $-CH_3$, $-OCH_3$, –OH, $-NH_2$, $-N(CH_3)_2$, –CN and $-NO_2$ *(ii)* R = –H, $-CH_3$, $-OCH_3$, –OH, $-NH_2$, $-N(CH_3)_2$, –CN and $-NO_2$, R′ = –H, *(iii)* R = R′ = –H, $-CH_3$, $-OCH_3$ –OH, $-NH_2$, $-N(CH_3)_2$, –CN and $-NO_2$. The torsion angles, $\alpha_{por\text{-}thio}$ and $\alpha_{per\text{-}thio}$, defined by 1-2-3-4 and 1-5-6-7, respectively.

3.1.3 Optimal structure of Por-Thio-Per derivatives.

Interest was focused to the derivatives with the following electron donating $-CH_3$, $-OCH_3$, $-OH$, $-NH_2$ and $-N(CH_3)_2$ and the electron withdrawing $-CN$ and $-NO_2$ groups. Starting from the optimal structure of Por-Thio-Per compound where $R = R' = -H$, the following derivatives were built, *(i)* $R = -H$, $R' = -CH_3$, $-OCH_3$ $-OH$, $-NH_2$, $-N(CH_3)_2$, $-CN$ and $-NO_2$ *(ii)* $R = -CH_3$, $-OCH_3$, $-OH$, $-NH_2$, $-N(CH_3)_2$, $-CN$ and $-NO_2$, $R' = -H$, *(iii)* $R = R' = -CH_3$, $-OCH_3$, $-OH$, $-NH_2$, $-N(CH_3)_2$, $-CN$ and $-NO_2$. Note that, the derivatives where $R \neq R'$ are not taken into account to simplify the data interpretation in the first place and, in addition, it is because asymmetric substitution on thiophene ring is synthetically complicated. To search for the most stable structure of these compounds, two steps of partial optimization were, subsequently applied. First, geometry of the substituted groups (while those of the other atoms were taken from 3.1.2 and kept constant throughout) were fully optimized. Then, the obtained geometry were fixed and the two torsion angles ($\alpha_{por\text{-}thio}$ and $\alpha_{per\text{-}thio}$) were adjusted in order to seek for the preferential conformation of the derivatives.

3.1.4 Optimal structure of Por-2Thio-Per and Por-3Thio-Per compound.

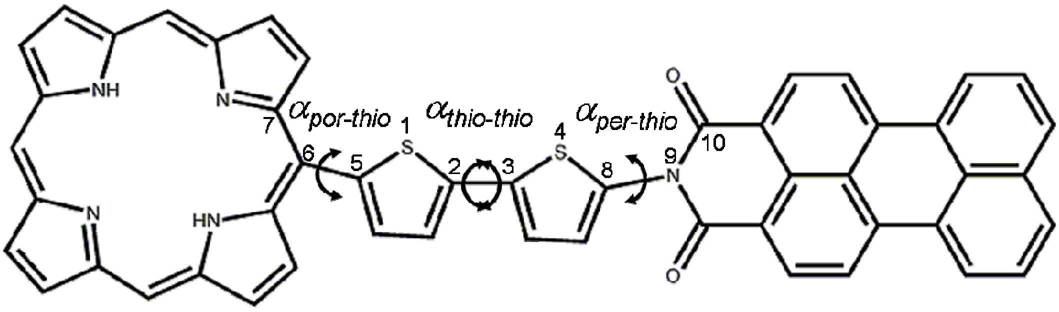

Figure 3.3. Two-dimensional structure of the Por-2Thio-Per compound where the torsion angle, $\alpha_{thio\text{-}thio}$, $\alpha_{por\text{-}thio}$, and $\alpha_{per\text{-}thio}$ defined by 1-2-3-4, 1-5-6-7 and 4-8-9-10, respectively.

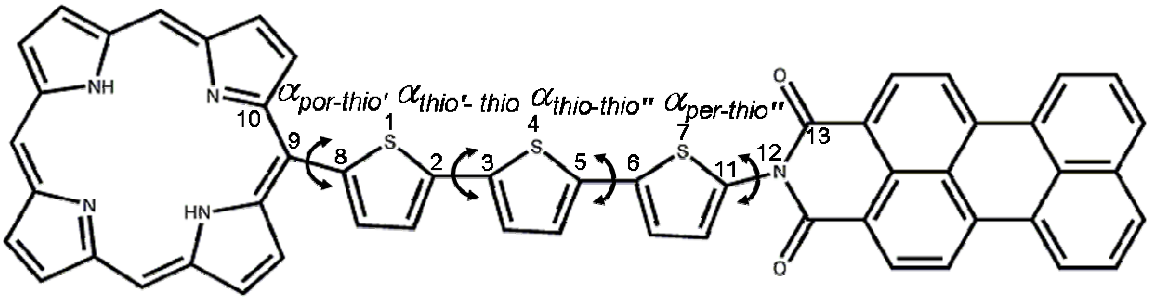

Figure 3.4. Two-dimensional structure of the Por-3Thio-Per compound where the torsion angle, $\alpha_{thio'\text{-}thio}$, $\alpha_{thio\text{-}thio''}$, $\alpha_{por\text{-}thio'}$, and $\alpha_{per\text{-}thio''}$ defined by 1-2-3-4, 4-5-6-7, 1-8-9-10, and 7-11-12-13, respectively.

For the Por-2Thio-Per compound, as there are more torsion angles related to the two thiophene units in comparison to those of Por-Thio-Per, it becomes more complicated to perform optimization manually. To avoid the difficulties, the following procedures were applied. *(i)* Thio-Thio compound was generated, then, $\alpha_{thio\text{-}thio}$ was scanned from 0˚ to 360˚ to seek the optimal angle. *(ii)* With the obtained optimal $\alpha_{thio\text{-}thio}$, two angles, $\alpha_{por\text{-}thio}$, and $\alpha_{per\text{-}thio}$ were subsequently, scanned in the manner as that applied for the Por-Thio-Per compound. The same procedures were also applied to seek for the optimal structure of the Por-3Thio-Per compound.

3.2 Optimal method for the electronic properties investigations.

With the optimal structure of the Por-Thio-Per and its derivatives obtained from 3.1.2 and 3.1.3, the B3LYP calculations at different basis sets: 6-31G(d), 6-31G(d,p), 6-31+G(g) and 6-31+G(d,p) have been performed. Seeking for compromising between the accuracy and the required computer time, the electronic properties of the calculated systems were used to validate the method applied. The resulting optimal method was, then, used for the investigated of electronic properties of the compound of interest throughout.

All calculations described in this chapter were carried out using Gaussian03 program package [41].

CHAPTER IV

RESULTS AND DISCUSSION

4.1 Structure and electronic properties of Por-Thio-Per compound and its derivatives.

4.1.1 Optimal structure of Por-Thio-Per compound.

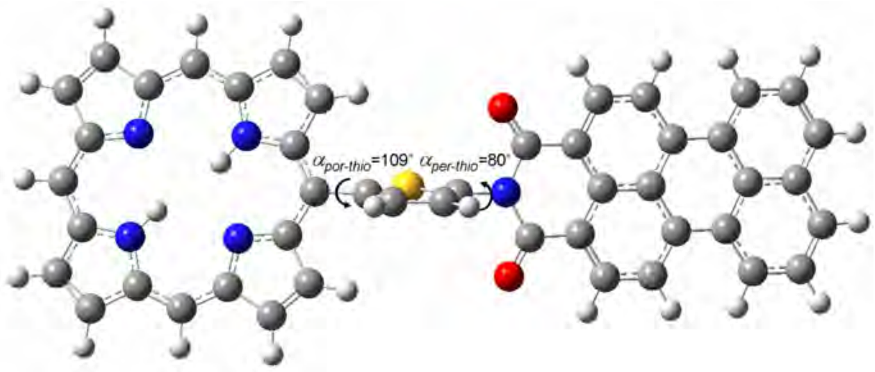

Figure 4.1. The optimal structure of the Por-Thio-Per compound (R = R′ = –H) where $\alpha_{por\text{-}thio}$ = 109° and $\alpha_{per\text{-}thio}$ = 80°, obtained from the B3LYP/6-31G(d) calculation.

With the fully optimization procedure and the B3LYP/6-31G(d) method, the calculated structure of the Por-Thio-Per compound where R = R′ = –H takes place at the torsion angles, $\alpha_{por\text{-}thio}$ and $\alpha_{per\text{-}thio}$ of 109° and 80°, respectively (Figure 4.1). In another approach, the potential energy surface, where $\alpha_{por\text{-}thio}$ and $\alpha_{per\text{-}thio}$ were optimized manually at the angle intervals 30^o, 5^o and 2^o were shown in Figures 4.2a, 4.2b and 4.2c, respectively. As shown in Figure 4.2c, the calculated energy minimum lies in the ranges of 106°-110° for $\alpha_{por\text{-}thio}$ and 80°-84° for $\alpha_{per\text{-}thio}$. Good agreement between the results yielded from the two optimized procedures indicates reliability of the obtained structure. Note that the obtained Por-Thio-Per geometries, bond lengths and angles, when R = R′ = –H were used and kept constant throughout in order to seek for the preferential torsion angles of its derivatives (see section 4.1.3 for details).

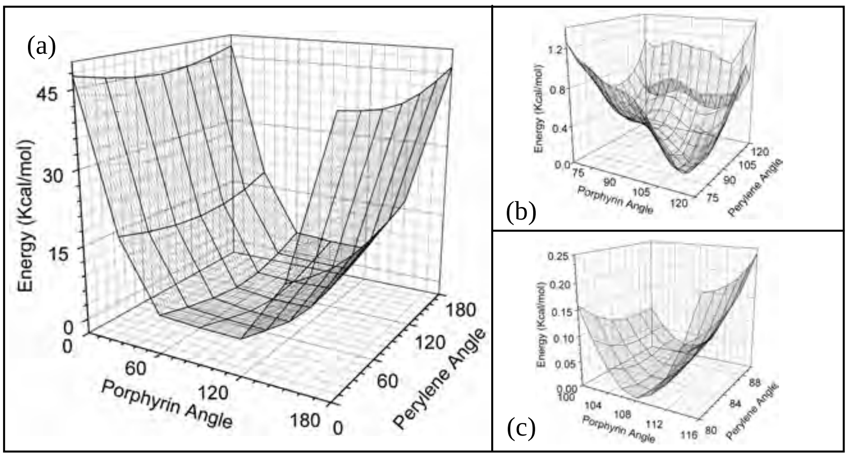

Figure 4.2. (a)-(c) potential energy surfaces of the Por-Thio-Per compound, where R = R′ = –H, as a function of the torsion angles ($\alpha_{por\text{-}thio}$ and $\alpha_{per\text{-}thio}$ defined in Figure 4.1) were optimized manually at the angle intervals 30°, 5° and 2°, respectively.

4.1.2 Optimal method for electronic properties investigations.

With the optimal configuration of the Por-Thio-Per (R = R′ = –H) compound where $\alpha_{por\text{-}thio}$ = 109° and $\alpha_{per\text{-}thio}$ = 80°, the B3LYP method at different sizes of the basis sets were applied to examine electronic properties of the investigated compound. This procedure was taken into account in order to seek the optimal level of accuracy compromising between reliability of the calculated results and CPU (Computation Processing Units) time needed. The HOMO, LUMO and energy gap as well as the required CPU times were summarized in Table 4.1. Examinations were also extended to the Por-Thio-Per and its derivatives where R = R′ = –OCH_3, –OH, –CN and –NO_2. The results were compared in Figure 4.3a-c.

As clearly seen from Table 4.1, significant differences of the HOMO and LUMO energies were yielded when the diffusion function, 6-31G+(d) and 6-31G+(d,p) were included. As expected, the absolute energies were found not to effect the HOMO-LUMO energy band gap significantly, 2.1619 eV, 2.1608 eV, 2.1149 eV and 2.1143 eV for the 6-31G(d) and 6-31G(d,p), 6-31G+(d) and 6-31G+(d,p) basis sets, respectively. These conclusions were also true for the selected Por-Thio-Per derivatives where the energy data were shown in Figure 4.3. Since the same level of accuracy has to be applied for all four derivatives defined in Figure 4.3 and the CPU time required to take into account the diffusion functions (6-31G+(d) and 6-31G+(d,p)) is dramatically higher than those of the other two basis sets, therefore, the B3LYP with the 6-31G(d) was chosen to be the optimal method for the electronic properties calculations for all compounds in this study.

Table 4.1 HOMO, LUMO, energy gap and CPU times obtained from the B3LYP method at different sizes of the basis sets for the Por-Thio-Per where R = R′ = –H, $\alpha_{por\text{-}thio}$ = 109° and $\alpha_{per\text{-}thio}$ = 80° (see Figure 4.1 for definition).

Method	HOMO (eV)	LUMO (eV)	Energy Gap (eV)	CPU time (hr:min)
B3LYP/6-31 G(d)	-5.030	-2.868	2.162	0:44
B3LYP/6-31 G(d,p)	-5.040	-2.880	2.160	0:51
B3LYP/6-31+ G(d)	-5.323	-3.208	2.115	9 :42
B3LYP/6-31+ G(d,p)	-5.334	-3.220	2.114	10:12

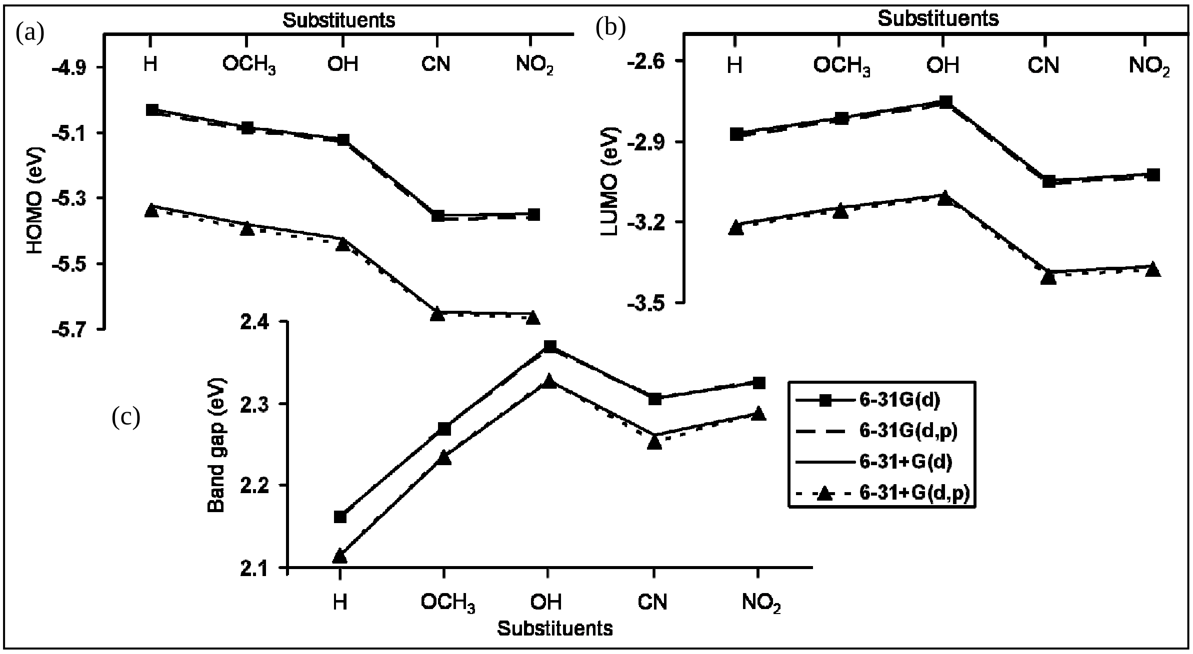

Figure 4.3. (a) HOMO, (b) LUMO and (c) energy gap of the Por-Thio-Per compound (where R = R′ = –H) and its derivatives (where R = R′ = –H, $-OCH_3$, –OH, –CN and $-NO_2$) calculated using the B3LYP method with different basis sets.

With the selected B3LYP 6-31G(d) calculation, the frontier molecular orbitals corresponding to the HOMO and LUMO energies for the most stable structure of the Por-Thio-Per compound where R = R′ = –H were visualized and shown in Figure 4.4. The HOMO energy was mapped to the porphyrin unit whereas the LUMO one was found to locate on the perylene unit, *i.e.*, the porphyrin and the perylene were assigned to act as the electron donor and electron acceptor, respectively. From the plots, electron transfer from porphyrin to perylene, which is the important feature for the electronic conductivity in solar cell application, was clearly visualized.

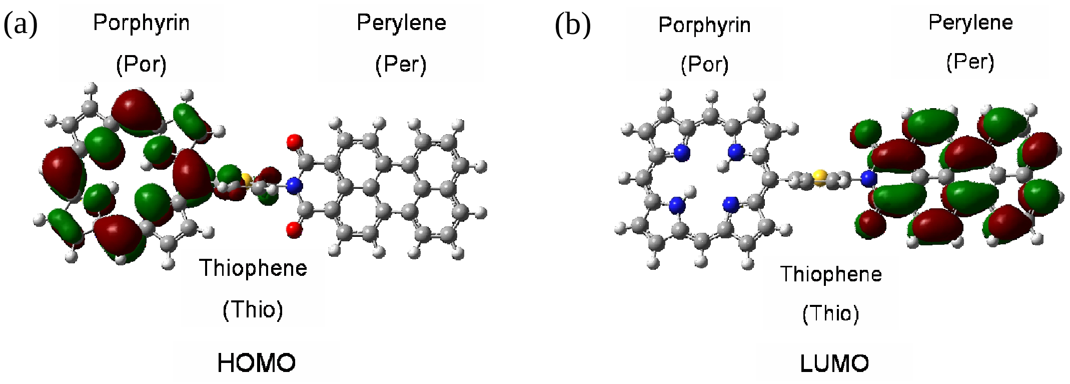

Figure 4.4. Frontier molecular orbital of (a) HOMO and (b) LUMO visualized by TD-B3LYP/6-31G(d) calculations indicated the electron donor and electron acceptor features of the porphyrin and perylene units, respectively.

4.1.3 Structural and electronic properties of Por-Thio-Per derivatives.

Table 4.2 Changes of the torsion angles ($\Delta\alpha_{por\text{-}thio}$ and $\Delta\alpha_{per\text{-}thio}$ defined in Figure 4.1) and the corresponding energy gap (ΔE_g) of the Por-Thio-Per derivatives obtained from the B3LYP/6-31G(d) calculations relative to those of the Por-Thio-Per compound (R = R′ = –H), subtract the values obtained from the Por-Thio-Per compound by those of its derivatives.

Substituent	Torsion angle (degree)			ΔE_g (eV)
R,R′	$\Delta\alpha_{por\text{-}thio}$	$\Delta\alpha_{per\text{-}thio}$	$\lvert\Delta\alpha_{per\text{-}thio} - \Delta\alpha_{por\text{-}thio}\rvert$	
Bi-substituent				
H,H	0	0	0	0.000
CH_3,CH_3	-7	4	11	0.019
OCH_3,OCH_3	-2	**20**	**22**	0.108
OH,OH	5	5	0	0.209
NH_2,NH_2	4	**-19**	**23**	-0.089
$N(CH_3)_2$, $N(CH_3)_2$	-1	8	9	-0.086
CN,CN	0	0	0	0.143
NO_2,NO_2	-7	6	13	0.164
Mono-substituent				
CH_3,H/H,CH_3	-6/4	3/-7	9/11	0.045/-0.051
OCH_3,H/H,OCH_3	0/2	1/5	1/3	**-0.157**/0.097
OH,H/H,OH	-1/0	0/0	1/0	**-0.157**/0.128
NH_2,H/**H,NH_2**	1/5	1/**-16**	0/**21**	-0.065/**-0.134**
$N(CH_3)_2$,H/H, $N(CH_3)_2$	2/3	6/3	4/0	**-0.118**/0.028
CN,H/H,CN	-3/0	-1/1	2/1	0.016/0.143
NO_2,H/H,NO_2	-3/2	1/4	4/2	-0.022/0.205

Referred to the calculation details given in section 3.1.3, changes of the torsion angles ($\Delta\alpha_{por\text{-}thio}$ and $\Delta\alpha_{per\text{-}thio}$ defined in Figure 4.1) and the corresponding energy gap (ΔE_g) of the Por-Thio-Per derivatives obtained from the B3LYP/6-31G(d) calculations relative to those of the Por-Thio-Per compound (R = R′ = –H) were extracted and summarized in Table 4.2. Here, the values obtained from the Por-Thio-Per compounds were subtracted by those of its derivatives. Therefore, negative value of the change of torsion angle denotes the rotation in the direction opposite to the arrow defined in Figure 4.1 whereas negative ΔE_g means that the newly designed derivative gives narrower energy gap and *vice versa*. In addition, absolute value of the $|\Delta\alpha_{per\text{-}thio} - \Delta\alpha_{por\text{-}thio}|$ implies the changes of the torsion angle between the two molecular planes of the porphyrin and perylene units.

In term of molecular structure, it is clearly seen from Table 4.2 that significant change of the torsion angle was found only for the two bi-substituted derivatives, R = R′ = $-OCH_3$ and $-NH_2$, and one mono-substituted derivative, R = –H and R′ = $-NH_2$ in which change of an angle between the porphyrin and perylene molecular planes ($|\Delta\alpha_{per\text{-}thio} - \Delta\alpha_{por\text{-}thio}|$) of >20^o (marked as bold characters in Table 4.2) was taken place. These findings can be described in terms of interaction between the substituted groups and one or both oxygen atoms of the perylene unit. Steric hindrance due to the $-OCH_3$ substituent repulses the oxygen atom of the perylene, leading to the positive $\Delta\alpha_{per\text{-}thio}$ (perylene was rotated in the direction of the arrow shown in Figure 4.1) by 20^o. This is not the case for the bi-substituted $-N(CH_3)_2$ in which repulsion between this bulky group and the two oxygen atoms of perylene (see also Figure 4.1) was observed to tilt the angle $\Delta\alpha_{per\text{-}thio}$ by only 8^o. For the $-NH_2$, the perylene unit was rotated by -19^o for the bi-substituted and -16^o for the mono-substituted due to a weak intramolecular hydrogen bond with one of the hydrogen atom of perylene. This hydrogen bond could not be formed for the –OH functional group because of the OH···O repulsion.

Interest was focused to the reduction of the HOMO-LUMO energy gap where the calculation results lead to the following conclusions. *(i)* The symmetric bi-substituent does not provide significantly lower of the ΔE_g, slightly narrower of the energy gaps of -0.089 eV and -0.086 eV were, however, observed for the derivatives where R = R′ = $-NH_2$ and $-N(CH_3)_2$, respectively. *(ii)* Noticeable changes of the HOMO-LUMO band gap were found for the four newly designed derivatives where

R,R′ = –OCH_3,–H; –OH,–H; –$N(CH_3)_2$,–H and –H,–NH_2 with the reduction of the ΔE_g by -0.157 eV, -0.157 eV, -0.118 eV and -0.134 eV, respectively. *(iii)* Decrease of the ΔE_g was significantly observed only when the substituents are electron donor groups. However, no relation was found between degree of electron donation and the ΔE_g reduction. *(iv)* Among the four highly potential candidates, three substitutions were found to take place at the porphyrine unit, R,R′ = –OCH_3,–H; –OH,–H and –$N(CH_3)_2$,–H.

As concluded in *(iii)* and *(iv)*, substitution of the electron donor group to the porphyrine unit was observed to be the favorable choice for the design of the new compounds for the dye-sensitized solar cells. This finding can be clearly understood by the frontier molecular orbital shown in Figure 4.4 (HOMO and LUMO orbitals) where the porphyrin unit was shown to serve as the electron donor. Therefore, increase of the electron density at this unit, due to the electron donor substituents, can directly facilitate the electron transfer to the perylene which is known to be a key factor for the dye-sensitized solar cells. However, this is not the case for what found for the mono-substituted –NH_2 at the perylene unit (R = –H and R′ = –NH_2) which lead also to decrease the energy gap by -0.134 eV (Table 4.2). The reason for this fact is due to the intramolecular hydrogen bond, which leads also to the change of the angle $\Delta\alpha_{per\text{-}thio}$ by -16^o as described above. This newly formed hydrogen bond was, then, assists the electron transfer to the perylene unit.

4.1.4 UV-visible spectra of the Por-Thio-Per derivatives.

Using the TD-B3LYP calculations in the Gaussion03 package, the UV-visible spectra for the investigated compounds were calculated. The obtained results for the free-base porphyrin, the free-base perylene, the Por-Thio-Per compound and the four newly designed derivatives were summarized in Figure 4.5.

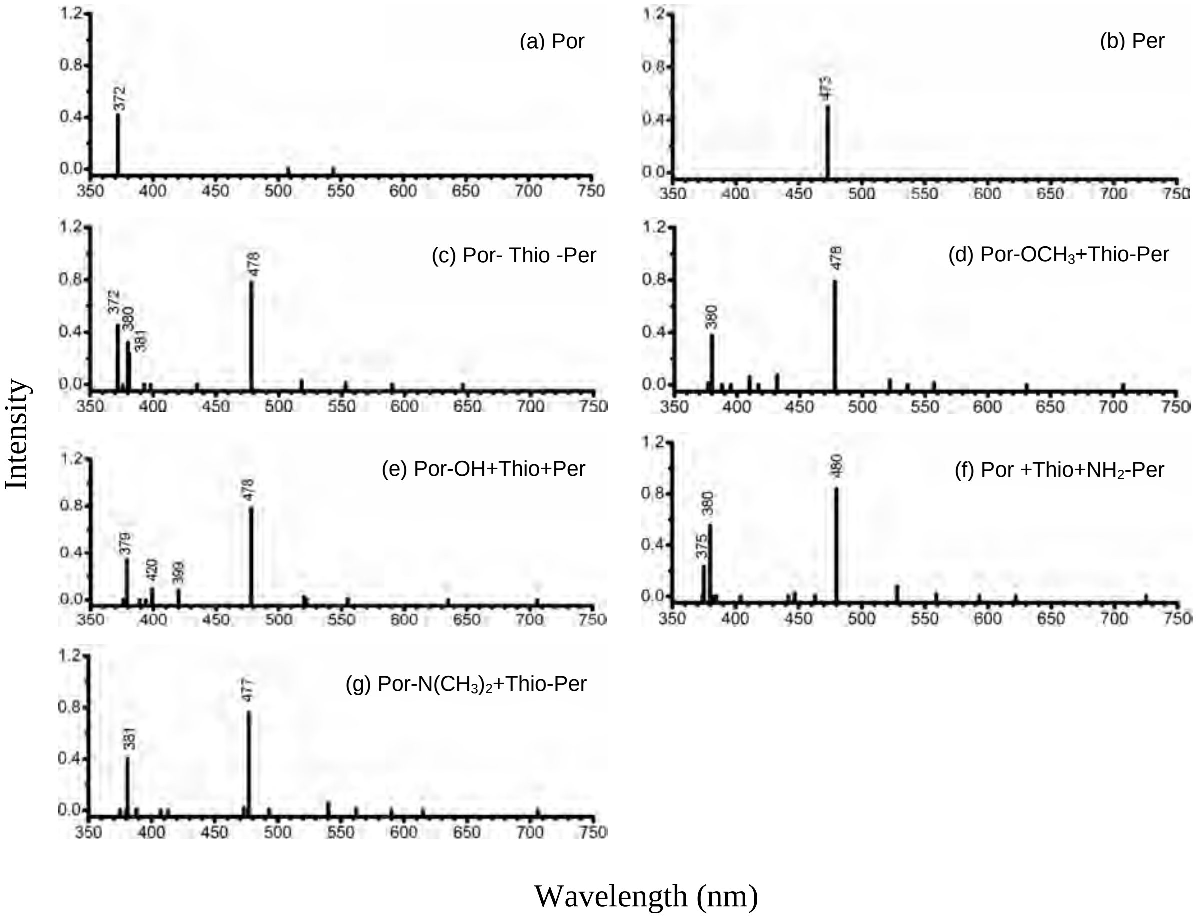

Figure 4.5. UV-visible spectra of the free base porphyrin, perylene, Por-Thio-Per compound (R = R´ = –H) and the four newly designed derivatives which provide significantly lower energy gap, relative to those of the Por-Thio-Per compounds (marked as bold characters in Table 4.2).

The free-base porphyrin shows maximum absorption spectra at 372 nm whereas the values for the perylene maximum at 473 nm (Figures 4.5a and b, respectively). The two calculated maxima, 372 and 473 nm, are in agreement with those yielded experimentally for the free-base porphyrin and perylene, respectively [7,8,9].

Several peaks were observed for the Por-Thio-Per compound (R = R´ = –H) and the four newly designed derivatives. It appears also that the absorption spectra of the Por-Thio-Per and its derivatives cover a broader range, 370-730 nm (Figures 4.5c-4.5g), compared to those between 372 nm and 473 nm for the two free bases (Figures 4.5a and 4.5b). The most important feature is that characteristics of the porphyrin and perylene molecules, which indicate by the absorptions spectra at 372 and 473 nm, remain unchanged. The first peak was only slightly shifted to 380 nm, 379 nm, 380 nm and 381 nm for the four derivatives, R = R´ = $-OCH_3$,–H; –OH,–H; –H,$-NH_2$ and $-N(CH_3)_2$,–H, respectively. The corresponding values for the second peaks of those derivatives are 478 nm, 478 nm, 480 nm and 477 nm, respectively.

4.2 Structure and electronic property of Por-Per, Por-2Thio-Per and Por-3Thio-Per compounds.

4.2.1 Optimal structure and electronic properties of Por-Per, Por-2Thio-Per and Por-3Thio-Per compounds.

With the calculation details given in chapter 3, the optimal structures of the investigated compounds obtained from the B3LYP/6-31G(d) calculations were shown in Figure 4.6. They, were, then, used for further examination of the electronic properties of the system.

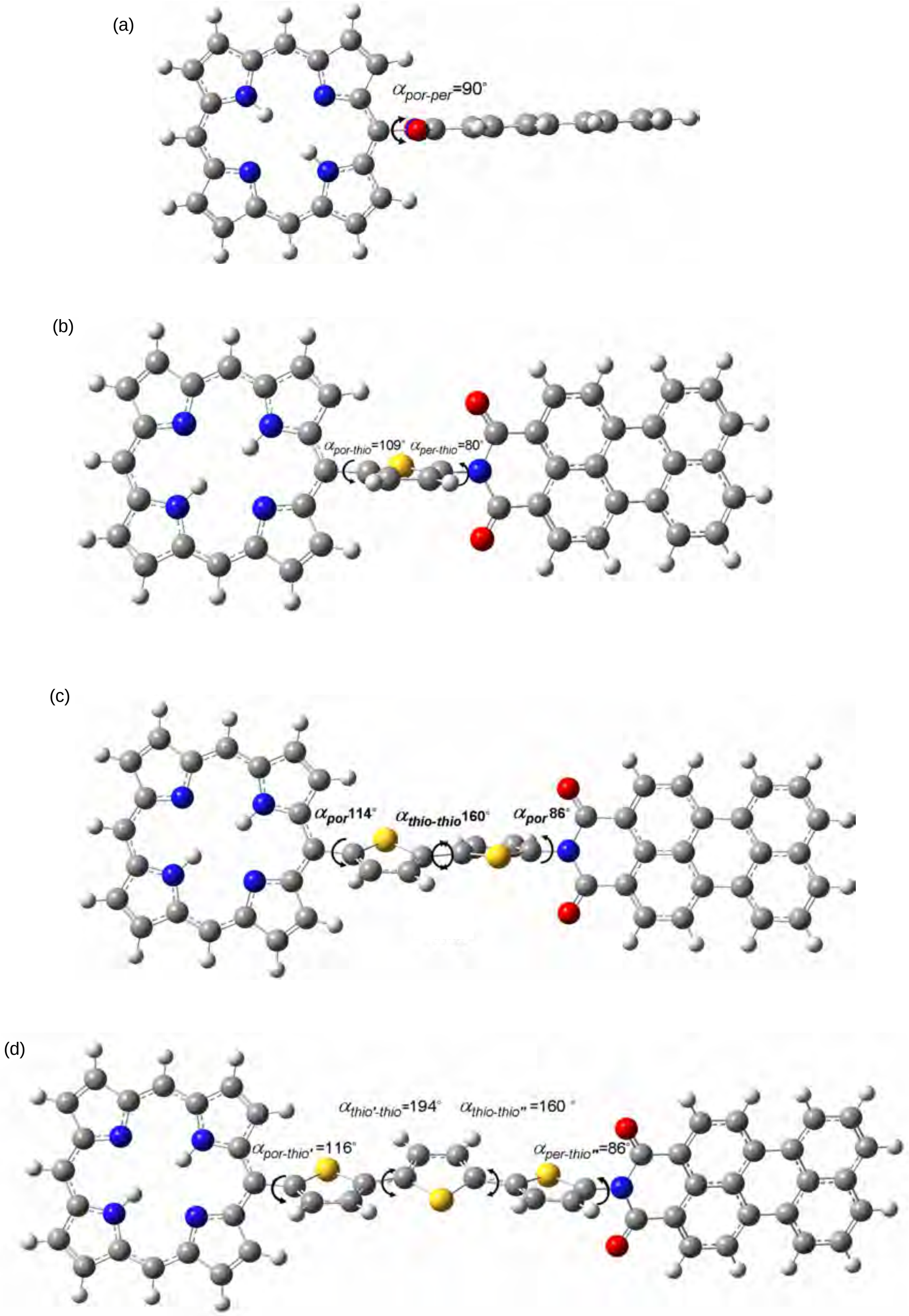

Figure 4.6. (a)-(d) the optimal structures for the Por-Per, Por-Thio-Per, Por-2Thio-Per and Por-3Thio-Per obtained from the B3LYP/6-31G(d) calculation.

Table 4.3 Changes of the torsion angles $\Delta\alpha_{por\text{-}thio}$ and $\Delta\alpha_{per\text{-}thio}$ and the corresponding energy gap (ΔE_g) of the Por-Per, Por-2Thio-Per and Por-3Thio-Per obtained from the B3LYP/6-31G(d) calculations relative to those of the Por-Thio-Per compound (R = R′ = –H), subtract the values obtained from the Por-Thio-Per compounds by those of Por-Per, Por-2Thio-Per and Por-3Thio-Per compounds. The E_g of Por-Per is 5.064 (eV).

Compound	No. of linker	Torsion angle (degree)			E_g (eV)	ΔE_g (eV)
		$\Delta\alpha_{por\text{-}thio}$	$\Delta\alpha_{per\text{-}thio}$	$\lvert\Delta\alpha_{per\text{-}thio} - \Delta\alpha_{por\text{-}thio}\rvert$		
Por-Thio-Per	1	0	0	0	2.162	0.000
Por-2Thio-Per	2	5	6	1	2.155	-0.007
Por-3Thio-Per	3	7	6	1	2.057	-0.105

The torsion angles, $\Delta\alpha_{por\text{-}thio}$ and $\Delta\alpha_{per\text{-}thio}$ as well as the corresponding energy gap (ΔE_g) of the Por-Per, Por-2Thio-Per, and Por-3Thio-Per compounds obtained from the B3LYP/6-31G(d) calculations relative to those of the Por-Thio-Per compound (R = R′ = –H) were extracted and summarized in Table 4.3. Here, the values obtained from the Por-Thio-Per compounds were subtracted by those of Por-Per, Por-2Thio-Per and Por-3Thio-Per compounds. The negative ΔE_g means that the designed compound gives less energy gap and *vice versa*. In addition, absolute value of the $\lvert\Delta\alpha_{per\text{-}thio} - \Delta\alpha_{por\text{-}thio}\rvert$ implies the changes of the torsion angle between two molecular planes of the porphyrin and perylene units.

With the porphyrin and perylene molecules, the direct integrating of two molecules yielded the Por-Per compound with the optimal $\alpha_{por\text{-}per}$ of 90°. The structure where the two molecular planes are perpendicular, lead to high steric hindrance and practically unpreferable to be used in dye-sensitized solar cell application. Moreover, the obtained HOMO-LUMO energy band gap of 5.064 eV is too high and makes the compound insulated. Therefore, the designation of new compound by introducing a good electron transferring linker such as thiophene is the promising way to improve efficiency of such material in dye-sensitized solar cell application. In terms of torsion angle, only slightly change was found in changing from Por-Thio-Per to Por-2Thio-Per and Por-3Thio-Per compounds (Table 4.3). This can be concluded that the thiophene linker does not decrease the steric effect of the structure of designed compound.

Theoretically, the HOMO-LUMO energy gap specifies the conductivity of material. The energy gap of higher than 4.0 eV is insulator. In this study, the calculated results lead to the following conclusions. *(i)* The Por-Per compound is insulator and provides significantly wider energy gap. *(ii)* Compared to Por-Thio-Per, the Por-2Thio-Per compound gives almost the same level of energy gap. *(iii)* Noticeable reduction of the HOMO-LUMO band gap was found for the Por-3Thio-Per compound, *i.e.*, it is -0.105 eV narrower that those of Por-Thio-Per. A conclusion is that the thiophene linker was found to facilitate electron transfer between the porphyrin and the perylene units.

4.2.2 UV-visible spectra and frontier molecular of the Por-Thio-Per compound.

The plot of calculated absorption spectra for free-base porphyrin (Por), perylene (Per), Por-Per, Por-Thio-Per, Por-2Thio-Per and Por-3Thio-Per compounds shown in Figures 4.7a-4.7e, respectively. The obtained peaks for the Por at 372 nm and the Per molecules at 473 nm are in good agreement with those yielded experimentally [7,8,9]. Several peaks were observed in absorption spectra of Por-Per, Por-Thio-Per, Por-2Thio-Per and Por-3Thio-Per compounds and where some of them show significantly strong. To understand the electronic properties in details, excitation states corresponding to the obtained spectra were examined.

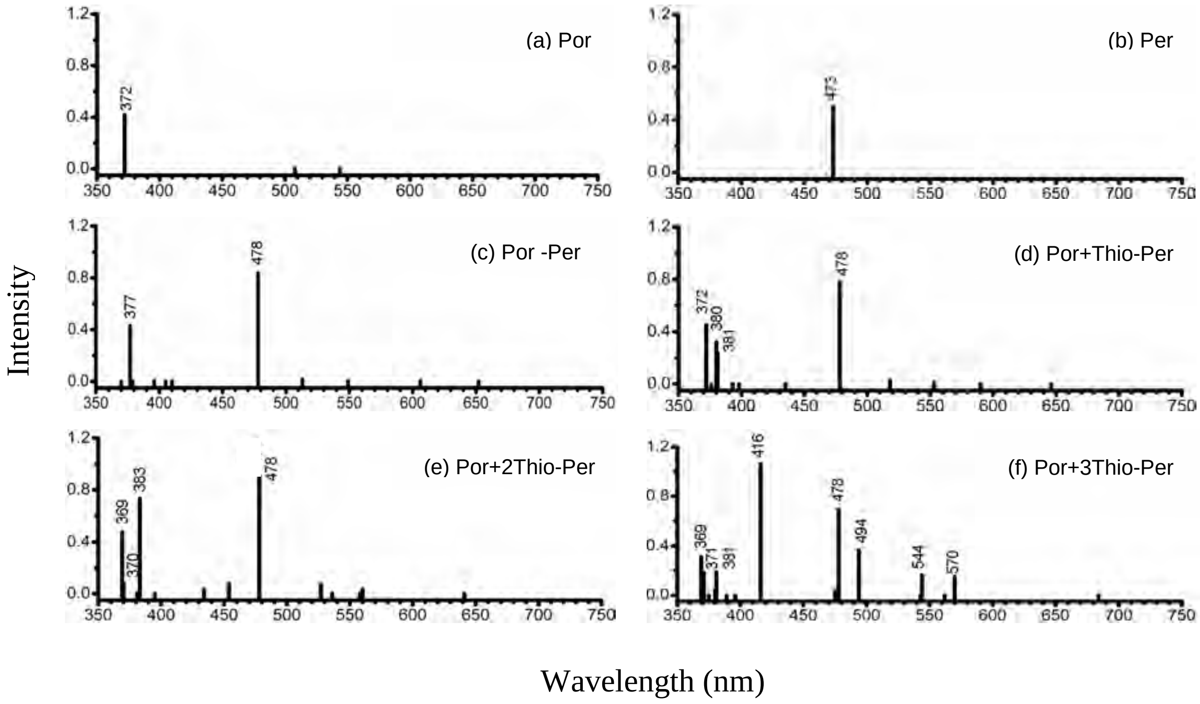

Figure 4.7. Absorption spectra of the (a) Por, (b) Per, (c) Por-Thio-Per, (d) Por-2Thio-Per compounds and (e) Por-3Thio-Per compound.

Frontier molecular orbital of Por-Thio-Per compound was summerized in Table 4.4. The visualization of frontier molecular orbital was demonstrated in Figure 4.8. Due to the orbital degeneracy, only 10 molecular orbitals among 11 excitations were shown. Nevertheless, the absorption spectra and corresponding frontier molecular orbitals of the Por-Per, Por-2Thio-Per and Por-3Thio-Per compounds were also calculated and given in appendix A.

Table 4.4 Electronic absorption spectra and frontier molecular orbital of Por-Thio-Per compound.

Excited state	Wavelength (nm)	Excitation	Frontier molecular orbital	Character of orbital
1	646	184→185	HOMO→LUMO	por→per
2	590	183→185	HOMO-1→LUMO	por→per
3,4		183→186	HOMO-1→LUMO+1	por
	553	183→187	HOMO-1→LUMO+2	por
	518	184→186	HOMO→LUMO+1	por
		184→187	HOMO→LUMO+2	por
5	478	182→185	HOMO-2→LUMO	per
6	435	179→185	HOMO-5→LUMO	por→per
		181→185	HOMO-3→LUMO	thio→ per
7	398	179→185	HOMO-5→LUMO	por→per
		180→185	HOMO-4→LUMO	por→per
8	393	182→186	HOMO-2→LUMO+1	per→por
9	381	179→186	HOMO-5→LUMO+1	por
		179→187	HOMO-5→LUMO+2	por
		180→186	HOMO-4→LUMO+1	por
		180→187	HOMO-4→LUMO+2	por
		182→187	HOMO-2→LUMO+2	per→por
		183→186	HOMO-1→LUMO+1	por
		183→187	HOMO-1→LUMO+2	por
		184→187	HOMO→LUMO+2	por
10	380	179→186	HOMO-5→LUMO+1	por
		179→187	HOMO-5→LUMO+2	por
		180→186	HOMO-4→LUMO+1	por
		180→187	HOMO-4→LUMO+2	por
		182→187	HOMO-2→LUMO+2	per→por
		183→186	HOMO-1→LUMO+1	por
		183→187	HOMO-1→LUMO+2	por
		184→186	HOMO→LUMO+1	por

Excited state	Wavelength (nm)	Excitation	Frontier molecular orbital	Character of orbital
11	376	184→187	HOMO→LUMO+2	por
		178→185	HOMO-6→LUMO	thio→per
		179→185	HOMO-5→LUMO	por→per
		180→185	HOMO-4→LUMO	por→per
		181→185	HOMO-3→LUMO	thio→per
		179→186	HOMO-5→LUMO+1	por
12	372	179→187	HOMO-5→LUMO+2	por
		181→186	HOMO-3→LUMO+1	thio→por
		183→186	HOMO-1→LUMO+1	por
		183→187	HOMO-1→LUMO+2	por
		184→186	HOMO→LUMO+1	por
		184→187	HOMO→LUMO+2	por

It can be seen from Figure 4.8 that the frontier molecular orbitals appear at three territories: *(i)* HOMO, HOMO-1, HOMO-4, HOMO-5, LUMO+1, LUMO+2, *(ii)* LUMO, HOMO-2 and *(iii)* HOMO-3, HOMO-6 take place at porphyrin unit, perylene unit and thiophene bridge, respectively. Derived from electron transpose, the HOMO-LUMO excitations can be classified into two types, where the excitation was created from the same and from different molecular units in the Por-Thio-Per compound, known as “specific” and “crossing” excitations, respectively.

The specific excitation corresponds to six excited states shown in Table 4.4. Those are excited states 3 and 4 of porphyrin generating the absorption spectra at 553 and 518 nm, respectively, and the excited states 9, 10 and 12 almost belong to porphyrin. The corresponding absorption spectra of the last three states are 381, 380, and 372 nm, respectively. Another specific excitation is the excited state 5 of perylene providing the absorption spectrum at 478 nm. The second excitation type, crossing, encoverage electron transfer between the following molecular units; porphyrin to perylene (por→per), perylene to porphyrin (per→por), thiophene to porphyrin (thio→por) and thiophene to perylene (thio→per). Obviously, electron can transfer from porphyrin to perylene through thiophene linker and yields the strongly absorption spectra at 478, 381, 380 and 372 nm, leading to an extended absorption range of 370-650 nm. It can be also seen in Table 4.4 that characteristics of porphyrin and perylene units which signified the absorptions spectra at 372 and 478 nm, respectively still remain.

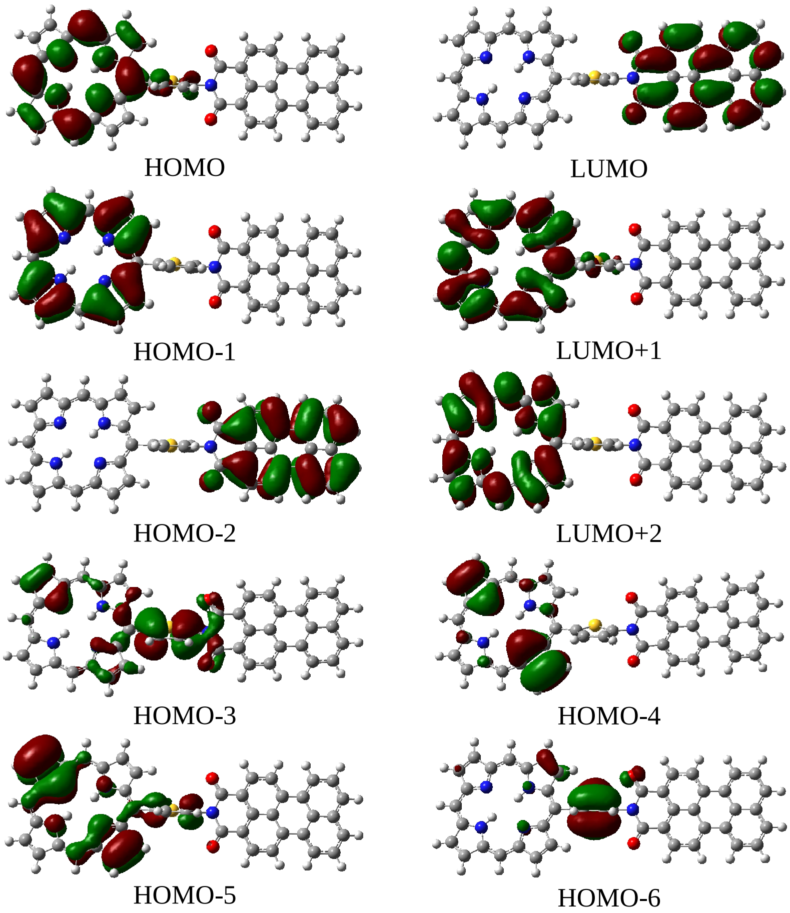
HOMO
LUMO
HOMO-1
LUMO+1
HOMO-2
LUMO+2
HOMO-3
HOMO-4
HOMO-5
HOMO-6

Figure 4.8. Visualized frontier molecular orbital for excitation of absorption spectra of Por-Thio-Per compound.

With the careful analysis of the excitations and corresponding frontier molecular orbitals of the Por-Per, Por-2Thio-Per and Por-3Thio-Per compounds, the obtained results are similar to those of the Por-Thio-Per (see appendix A). Transferring of electron from the porphyrin to the perylene units which is the essential feature in solar cell application was found and the characteristics of the free-base porphyrin and perylene at 369 and 478 nm, respectively, are unchanged. In calculation, oligo-thiophene chromophore shows their characteristic absorption behavior and plays role in orbital excitation.

CHAPTER V

CONCLUSIONS

The B3LYP/6-31G(d) calculation was found to be the suitable compromising method between accuracy and computational time required to seek for the optimal structure and electronic properties of Por-Per, Por-Thio-Per, Por-2Thio-Per, and Por-3Thio-Per compounds. The molecular design by integrating of porphyrin and perylene units using the thiophene linkage was proposed to be the alternative way to improve the performance of organic-based material in solar cell application. The excited states and corresponding frontier molecular orbitals as well as the absorption spectra of Por-Per, Por-Thio-Per, Por-2Thio-Per, and Por-3Thio-Per were studied and visuallized using the TD-B3LYP with 6-31G(d) level of accuracy. The investigated compounds were observed to enhance the absorption spectra in range of 370-690 nm without disturbing characteristic spectra of the free-base porphyrin and perylene units. Moreover, the visualization of the HOMO-LUMO frontier molecular orbital of these compounds clearly demonstrates the electron transfer from porphyrin to perylene units.

The Por-Thio-Per derivatives were designed from the Por-Thio-Per compound in the manner of bi- and mono- substitution R at C3 and R' at C4 of the thiophene linker where two properties, torsion angle and band gap energy were investigated. The bi-substituent, ($–OCH_3$,$–OCH_3$; $–NH_2$,$–NH_2$) and mono-substituent (–H,$–NH_2$), lead to significant changes of the torsion angles due to steric effects and intramolecular hydrogen bond. It was also found that the band gap energy of mono-substituent where R, R' = $–OCH_3$,–H; –OH,–H; –H,$–NH_2$ and $–N(CH_3)_2$,–H were significatly decreased. This is due to the electron donating and electron withdrawing effects. The Por-Thio-Per compound and the four newly designed Por-Thio-Per derivatives can enhance the absorption spectra to the range 370-730 nm and the characteristic absorption behavior of each chromophore still exists. Apparently, the electron transfer from porphyrin to perylene units, which is necessary for solar cell application, was obviously observed.

REFERENCES

[1] Guenes, S.; Sariciftci, N. S., Hybrid solar cells. *Inorg.Chim. Acta*. 361 (2008): 581-588.

[2] O'Regan, B.; Grätzel, M., A low-cost, high-efficiency solar cell based on dye-sensitized colloidal TiO_2 films. *Nature*. 353 (1991): 737-740.

[3] Grätzel, M., Photoelectrochemical cells. *Nature*. 414 (2001): 338-344.

[4] Cass, M. J.; Qiu, F. L.; Walker, A. B.; Fisher, A. C.; Peter, L. M., Influence of grain morphology on electron transport in dye sensitized nanocrystalline solar cells. *The J. Phys. Chem. B*. 107 (2003): 113-119.

[5] Brabec, C. J.; Sariciftci, N. S.; Hummelen, J. C., Plastic solar cells. *Adv. Funct. Mater*.11 (2001): 15-26.

[6] Nunzi, J.-M., Organic photovoltaic materials and devices. *C. R. Phys*. 3 (2002): 523-542.

[7] Gouterman, M. *The porphyrins*. Academic Press. Inc, 1978.

[8] Sundholm, D., Interpretation of the electronic absorption spectrum of free-base porphin using time-dependent density-functional theory. *Phys. Chem. Chem. Phys.* 2 (2000): 2275 - 2281.

[9] Prathapan, S.; Yang, S. I.; Seth, J.; Miller, M. A.; Bocian, D. F.; Holten, D.; Lindsey, J. S., Synthesis and excited-state photodynamics of perylene porphyrin dyads. 1. parallel energy and charge transfer via a diphenylethyne linker. *J. Phys. Chem. B*. 105 (2001): 8237-8248.

[10] Choi, H.; Lee, J. K.; Song, K.; Kang, S. O.; Ko, J., Novel organic dyes containing bis-dimethylfluorenyl amino benzo[b]thiophene for highly efficient dye-sensitized solar cell. *Tetrahedron*. 63 (2007): 3115-3121.

[11] Sanghoon, K.; Hyunbong, C.; Chul, B.; Kihyung, S.; Kang, S. O.; Jaejung, K., Synthesis of conjugated organic dyes containing alkyl substituted thiophene for solar cell. *Tetrahedron*. 63 (2007): 11436-11443.

[12] Schropp, R. E. I.; Zeman, M., *Amorphous and microcrystalline silicon solar cells modeling, materials, and device technology*. Springer**,** 1998.

[13] Green, M. A., *Power to the people: sunlight to electricity using solar cells*. UNSW Press, 2000.

[14] Anderson, B., Materials availability for large-scale thin-film photovoltaics. *Prog. Photovoltaics Res. Appl*. 8 (2000): 61-76.

[15] Green, M. A., Third generation photovoltaics: ultra-high conversion efficiency at low cost. *Prog. Photovoltaics Res. Appl*. 9 (2001): 123-135.

[16] Grätzel, M.; , Conversion of sunlight to electric power by nanocrystalline dye-sensitized solar cells. *J. Photochem. Photobiol. A*. 164 (2004): 3-14.

[17] Wasielewski, M. R., Photoinduced electron transfer in supramolecular systems for artificial photosynthesis. *Chem. Rev*. 92 (1992): 435-461.

[18] Battersby, A. R.; Fookes, C. J. R.; Matcham, G. W. J.; Mcdonald, E., Photoinduced electron transfer in supramolecular systems for artificial photosynthesis. *Chem. Rev*. 92 (1992): 435-461.

[19] Je, F., *Porphyrins and metalloporphyrins; their general, physical and coordination chemistry, and laboratory methods*. Elsevier: Amsterdam, 1964.

[20] Donaldson, D. M.; Robertson, J. M.; White, J., The crystal and molecular structure of perylene. *Proc. R. Soc. Lond. A Math. Phys. Sci*. 220 (1953): 311-321.

[21] Roncali, J., Conjugated poly(thiophenes): synthesis, functionalization, and applications. *Chem. Rev*. 4 (1992): 711-738.

[22] Chan, H. S. O.; Ng, S. C., Synthesis, characterization and applications of thiophene-based functional polymers. *Prog. Polym. Sci*. 23 (1998): 1167-1231.

[23] Jérome, B.; Stéphanie, L.-L.; Nuria, G.-P.; Piétrick, H., correlation of electrochemical and theoretical parameters in perylenediimide-[60]fullerene dyads. *Theochem*. 815 (2007): 145-150.

[24] Hara, K.; Miyamoto, K.; Abe, Y.; Yanagida, M., Electron transport in coumarin-dye-sensitized nanocrystalline TiO_2 electrodes. *J. Phys. Chem. B*. 109 (2005): 23776-23778.

[25] De, A. K.; Ganguly, T., Theoretical predictions for occurrence of charge transfer complex within the two synthesized bichromophores considering the role oftheir spacers in interactions with the p-orbitals of the redox centers. *Chem. Phys. Lett*. 428 (2006): 213-219.

[26] Muhlbacher, D.; Scharber, M.; Morana, M.; Zhu, Z.; Waller, D.; Gaudiana, R.; Brabec, C., High photovoltaic performance of a low-bandgap polymer. *Adv. Mater*. 18 (2006): 2884-2889.

[27] Nilsing, M.; Persson, P.; Lunell, S.; Ojamae, L., Dye-sensitization of the TiO_2 rutile (110) surface by perylene dyes: quantum-chemical periodic B3LYP computations. *J. Phys. Chem. C*. 111 (2007): 12116-12123.

[28] Schrödinger, E., Quantisierung als eigenwertproblem. *Ann. Phys*. 79 (1926): 361-376.

[29] Levin, I. N., *Quantum chemistry*. (5th ed.), University of New York: Prentice Hall, 2000.

[30] Cramer, C. J., *Essentials of computational chemistry*. University of Minnesotac: John Wiley & Sons, Ltd., 2002.

[31] Schrödinger, E., An undulatory theory of the mechanics of atoms and molecules. *Phys. Rev*. 28 (1926): 1049-1070.

[32] Szabo, A.; Ostlund, N. S., *Modern quantum chemistry introduction to advanced electronic structure theory*. (1st ed.), USA, Mcgraw-Hill, 1989.

[33] Cramer, C. J., *Essentials of computational chemistry*. Chichester: John Wiley & Sons, Ltd., 2002.

[34] Parr, R. G.; Yang, W., *Density functional theory of atoms and molecules*. New York**:** Oxford University Press, 1989.

[35] Lee, C.; Yang, W.; Parr, R. G., Development of the collesalvetti correlation-energy formula into a functional of the electron density. *Phys. Rev*. 37 (1988): 785-789.

[36] Beck, A. D., Density-functional thermochemistry. III. The role of exact exchange. *Chem. Phys*. 98 (1993): 5648-5652.

[37] Jensen, F., *Introduction to computational chemistry*. (2nd ed.), University of Southern Denmark: John Wiley & Sons Ltd., 2007.

[38] Jamorski, C.; Casida, M. E.; Salahub, D. R., Dynamic polarizabilities and excitation spectra from a molecular implementation of time-dependent density-functional response theory: N_2 as a case study. *J. Chem. Phys.* 104 (1996): 5134-5147.

[39] Runge, E.; Gross, E. K. U., Density-functional theory for time-dependent systems. *Phys. Rev. Lett.* 52 (1984): 997-1000.

[40] Casida, M. E., *In recent advances in computational chemistry*. (1st ed.), Singapore: World Scientific, 1995.

[41] Frisch, M. J., et al. *Gaussian 03, Revision C.02*. Gaussian, Inc., 2004.

[42] Okuno, Y.; Kamikado, T.; Yokoyama, S.; Mashiko, S., Theoretical study of aryl-ring rotation in arylporphyrins. *Theochem.* 594 (2002): 55-60.

[43] Okuno, Y.; Kamikado, T.; Yokoyama, S.; Mashiko, S., Determining the conformation of a phenylene-linked porphyrin dimer by NMR spectroscopy and quantum chemical calculations. *Theochem.* 631 (2003): 13-20.

[44] Earles, J. C.; Gordon, K. C.; Officer, D. L.; oligomers, P. W., A spectroscopic and computational study of the neutral and radical cation species of conjugated aryl-substituted 2,5-bis(2-thien-2-ylethenyl)thiophene-based *J. Phys. Chem. A.* 111 (2007): 7171-7180.

[45] Estrada, L. A.; Montes, V. A.; Zyryanov, G.; Anzenbacher, P., Triplet energy studies of thiophene and para-phenylene based oligomers. *J. Phys. Chem. B.* 111 (2007): 6983-6986.

[46] Yu Chen, Y. L.; EI-Khouly, M. E.; Zhuang, X.; Araki, Y.; Ito, O.; Zhang, W., Supramolecular zinc phthalocyanine perylene bisimide triad: synthesis and photophysical properties. *J. Phys. Chem. C.* 111 (2007): 16096 -16099.

[47] Hagberg, D. P.; Edvinsson, T.; Marinado, T.; Boschloo, G.; Hagfeldt, A.; Sun, L., A novel organic chromophore for dye-sensitized nanostructured solar cells. *Chem. Commun.* 2006: 2245-2247.

[48] Petsalakis, I. D.; Tagmatarchis, N.; Theodorakopoulos, G., Theoretical study of fulleropyrrolidines by density functional and time-dependent density functional theory. *J. Phys. Chem. C.* 111 (2007): 4139-14149.

[49] Zhang, X.; Zhang, J.-J.; Xia, Y.-Y., Molecular design of coumarin dyes with high efficiencyin dye-sensitized solar cells. *J. Photochem. Photobiol. A* 194 (2008): 167-172.

APPENDICES

APPENDIX A

Electronic absorption spectra and frontier molecular
orbital of Por-Per, Por-2Thio-Per and Por-3Thio-Per compounds result.

Table A.1 Electronic absorption spectra and frontier molecular orbital of Por-Per compound.

Excited state	Wavelength (nm)	Excitation	Frontier molecular orbital	Character of orbital
1	652	163→164	HOMO→LUMO	por→per
2	606	162→164	HOMO-1→LUMO	por→per
3,4	549 513	162→165	HOMO-1→LUMO+1	por
		162→166	HOMO-1→LUMO+2	por
		163→165	HOMO→LUMO+1	por
		163→166	HOMO→LUMO+2	por
5	478	150→167	HOMO-13→LUMO+3	per
		161→164	HOMO-2→LUMO	per
6	410	161→165	HOMO-2→LUMO+1	per→por
7	405	159→164	HOMO-4→LUMO	por→per
		160→164	HOMO-3→LUMO	por→per
8	396	161→166	HOMO-2→LUMO+2	per→por
9	379	158→164	HOMO-5→LUMO	por+per→per
		159→164	HOMO-4→LUMO	por→per
		160→164	HOMO-3→LUMO	por→per
10	377	159→165	HOMO-4→LUMO+1	por
		159→166	HOMO-4→LUMO+2	por
		160→165	HOMO-3→LUMO+1	por
		162→165	HOMO-1→LUMO+1	por
		162→166	HOMO-1→LUMO+2	por
		163→165	HOMO→LUMO+1	por
		163→166	HOMO→LUMO+2	por
11	370	157→164	HOMO-6→LUMO	por+per →per
		158→164	HOMO-5→LUMO	por+per→per
		158→168	HOMO-5→LUMO+4	por+per →per
		159→164	HOMO-4→LUMO	por→per

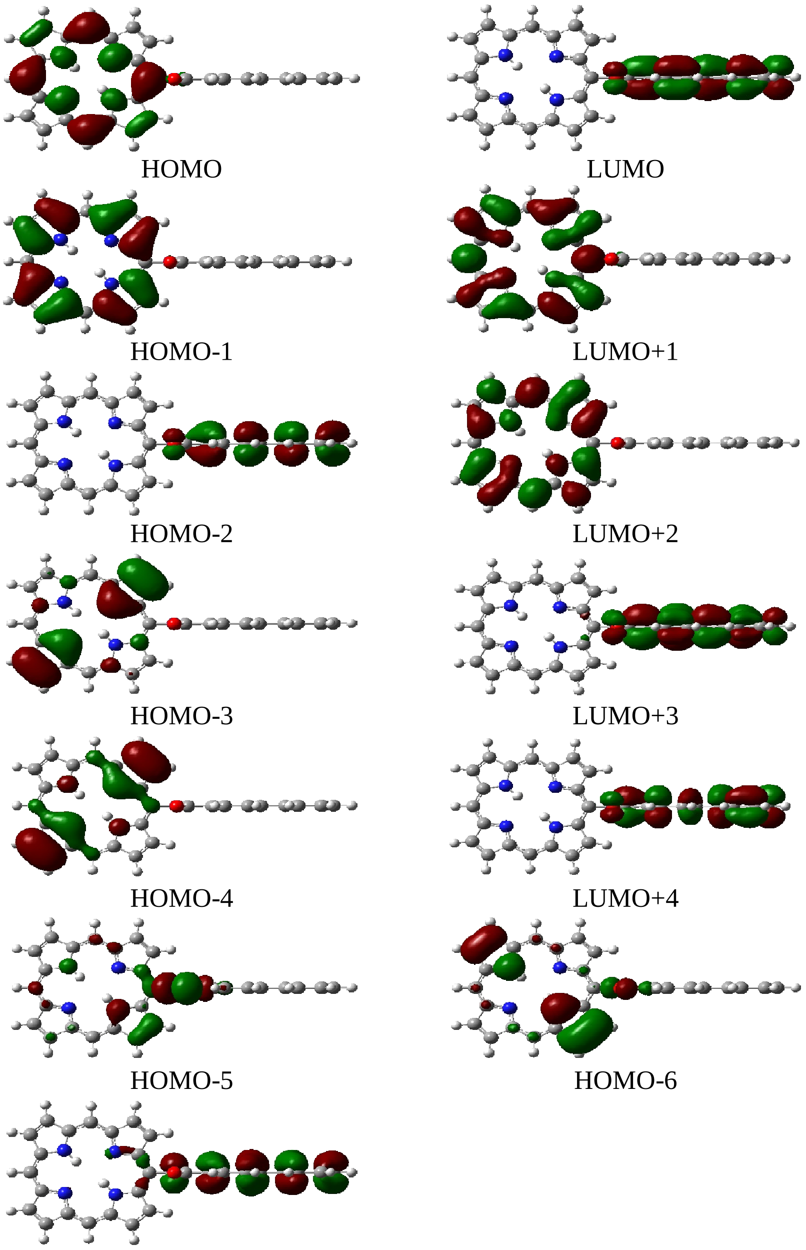

HOMO LUMO

HOMO-1 LUMO+1

HOMO-2 LUMO+2

HOMO-3 LUMO+3

HOMO-4 LUMO+4

HOMO-5 HOMO-6

HOMO-13

Figure A.1 Visualized frontier molecular orbital for excitation of absorption spectra of Por-Per compound.

Table A.2 Electronic absorption spectra and frontier molecular orbital of Por-2Thio-Per compound.

Excited state	Wavelength (nm)	Excitation	Frontier molecular orbital	Character of orbital
1,4	641	203→206	HOMO-2→LUMO	por+thio→per
	536	205→206	HOMO→LUMO	por+thio→per
2,5		204→207	HOMO-1→LUMO+1	por
	560	204→208	HOMO-1→LUMO+2	por
	527	205→207	HOMO→LUMO+1	por+thio→por
		205→208	HOMO→LUMO+2	por+thio→por
3	558	204→206	HOMO-1→LUMO	por→per
6	478	202→206	HOMO-3→LUMO	per
		203→207	HOMO-2→LUMO+1	por+thio→por
7	454	202→206	HOMO-3→LUMO	per
		203→207	HOMO-2→LUMO+1	por+thio→por
		204→208	HOMO-1→LUMO+2	por
		205→207	HOMO→LUMO+1	por+thio→por
8	434	203→208	HOMO-2→LUMO+2	por+thio→por
		204→207	HOMO-1→LUMO+1	por
		205→208	HOMO→LUMO+2	por+thio→por
9	395	202→207	HOMO-3→LUMO+1	per→por
10	383	200→207	HOMO-5→LUMO+1	por
		200→208	HOMO-5→LUMO+2	por
		201→207	HOMO-4→LUMO+1	por
		203→207	HOMO-2→LUMO+1	por+thio→por
		203→208	HOMO-2→LUMO+2	por+thio→por
		204→207	HOMO-1→LUMO+1	por
		204→208	HOMO-1→LUMO+2	por
		205→207	HOMO→LUMO+1	por+thio→por
		205→208	HOMO→LUMO+2	por+thio→por
		205→209	HOMO→LUMO+3	por+thio→per+thio
		205→210	HOMO→LUMO+4	por+thio→per+thio

Excited state	Wavelength (nm)	Excitation	Frontier molecular orbital	Character of orbital
11	382	201→206	HOMO-4→LUMO	por→per
12	381	202→208	HOMO-3→LUMO+2	per→ por
13	370	191→206	HOMO-14→LUMO	por+thio+per→per
		196→206	HOMO-9→LUMO	por+ per→per
		197→206	HOMO-8→LUMO	por+thio+per→per
		198→206	HOMO-7→LUMO	thio→per
		199→206	HOMO-6→LUMO	thio→per
		200→206	HOMO-5→LUMO	por→per
		205→209	HOMO→LUMO+3	por+thio→per+thio
		205→210	HOMO→LUMO+4	por+thio→per+thio
14	369	197→206	HOMO-8→LUMO	por+thio+per→per
		199→206	HOMO-6→LUMO	thio→per
		200→208	HOMO-5→LUMO	por→per
		201→208	HOMO-4→LUMO+2	por
		203→208	HOMO-2→LUMO+2	por+thio→por
		204→207	HOMO-1→LUMO+1	por
		204→208	HOMO-1→LUMO+2	por
		205→208	HOMO→LUMO+2	por+thio→por
		205→209	HOMO→LUMO+3	por+thio→per+thio
		205→210	HOMO→LUMO+4	por+thio→per+thio

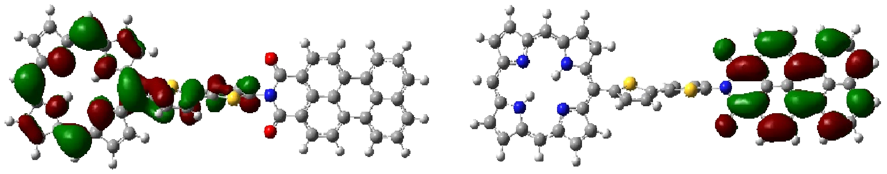

HOMO LUMO

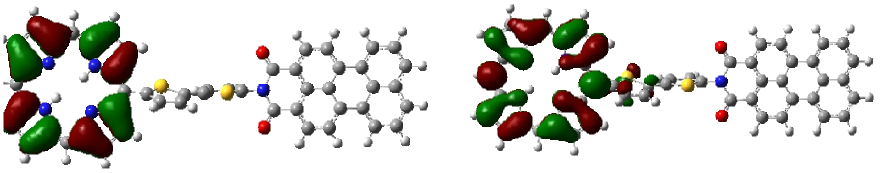

HOMO-1 LUMO+1

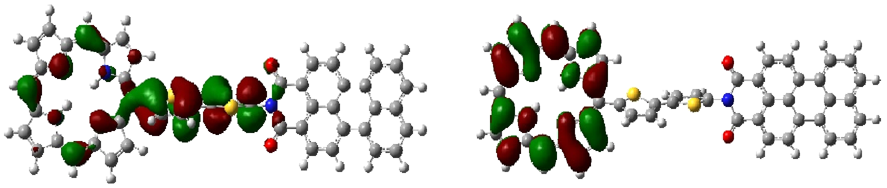

HOMO-2 LUMO+2

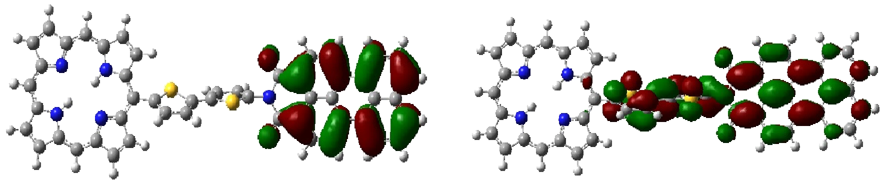

HOMO-3 LUMO+3

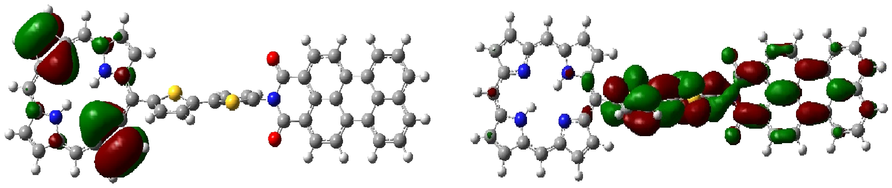

HOMO-4 LUMO+4

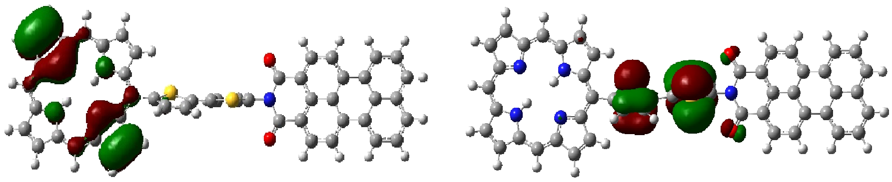

HOMO-5 HOMO-6

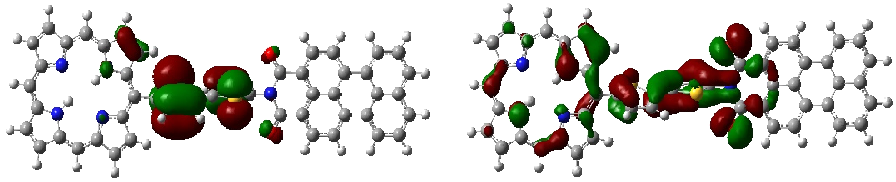

HOMO-7 HOMO-8

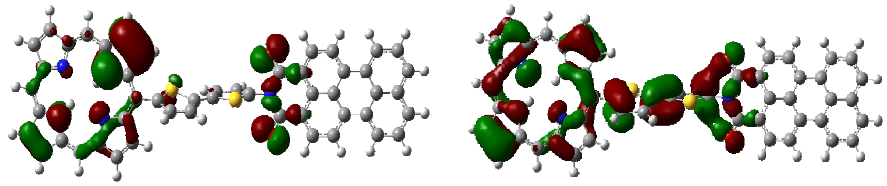

HOMO-9 HOMO-14

Figure A.2 Visualized frontier molecular orbital for excitation of absorption spectra of Por-2Thio-Per compound.

Table A.3 Electronic absorption spectra and frontier molecular orbital of Por-3Thio-Per compound.

Excited state	Wavelength (nm)	Excitation	Frontier molecular orbital	Character of orbital
1,3	684 562	224→227	HOMO-2→LUMO	por+thio→per
		225→227	HOMO-1→LUMO	por+thio→per
		226→227	HOMO→LUMO	por+thio→per
2	570	224→228	HOMO-2→LUMO+1	por+thio→por
		225→228	HOMO-1→LUMO+1	por+thio→por
		225→229	HOMO-1→LUMO+2	por+thio→por
		226→228	HOMO→LUMO+1	por+thio→por
		226→229	HOMO→LUMO+2	por+thio→por
4	544	224→228	HOMO-2→LUMO+1	por+thio→por
		224→229	HOMO-2→LUMO+2	por+thio→por
		225→228	HOMO-1→LUMO+1	por+thio→por
		226→228	HOMO→LUMO+1	por+thio→por
		226→229	HOMO→LUMO+2	por+thio→por
5	543	224→227	HOMO-2→LUMO	por+thio→per
		225→227	HOMO-1→LUMO	por+thio→per
6	494	223→227	HOMO-3→LUMO	per
		224→228	HOMO-2→LUMO+1	por+thio→por
		224→230	HOMO-2→LUMO+3	por+thio→por
		225→228	HOMO-1→LUMO+1	por+thio→por
		225→229	HOMO-1→LUMO+2	por+thio→por
		226→228	HOMO→LUMO+1	por+thio→por
		226→229	HOMO→LUMO+2	por+thio→por
7	478	223→227	HOMO-3→LUMO	per
		224→230	HOMO-2→LUMO+3	por+thio→por
		225→228	HOMO-1→LUMO+1	por+thio→por
		226→230	HOMO→LUMO+3	por+thio→thio

Excited state	Wavelength (nm)	Excitation	Frontier molecular orbital	Character of orbital
8	475	223→227	HOMO-3→LUMO	per
		224→228	HOMO-2→LUMO+1	por+thio→por
		224→230	HOMO-2→LUMO+3	por+thio→por
		225→228	HOMO-1→LUMO+1	por+thio→por
		225→229	HOMO-1→LUMO+2	por+thio→por
		226→229	HOMO→LUMO+2	por+thio→por
9	416	224→230	HOMO-2→LUMO+3	por+thio→thio
		225→228	HOMO-1→LUMO+1	por+thio→por
		226→230	HOMO→LUMO+3	por+thio→thio
10	396	223→228	HOMO-3→LUMO+1	per→por
11	389	216→227	HOMO-10→LUMO	per+thio→per
		220→227	HOMO-6→LUMO	por+thio→per
		221→227	HOMO-5→LUMO	por+thio→per
		222→227	HOMO-4→LUMO	por→per
12	381	220→228	HOMO-6→LUMO+1	por+thio→por
		220→229	HOMO-6→LUMO+2	por+thio→por
		221→228	HOMO-5→LUMO+1	por+thio→por
		221→229	HOMO-5→LUMO+2	por+thio→por
		222→228	HOMO-4→LUMO+1	por
		223→229	HOMO-3→LUMO+2	per→por
		224→228	HOMO-2→LUMO+1	por+thio→por
		224→229	HOMO-2→LUMO+2	por+thio→por
		224→230	HOMO-2→LUMO+3	por+thio→thio
		225→228	HOMO-1→LUMO+1	por+thio→por
		225→229	HOMO-1→LUMO+2	por+thio→por
		225→230	HOMO-1→LUMO+3	por+thio→thio
		226→229	HOMO→LUMO+2	por+thio→por
		226→230	HOMO→LUMO+3	por+thio→thio
13	380	223→229	HOMO-3→LUMO+2	per→por
		224→230	HOMO-2→LUMO+3	por+thio→thio

Excited state	Wavelength (nm)	Excitation	Frontier molecular orbital	Character of orbital
14	375	221→227	HOMO-5→LUMO	por+thio→per
		222→227	HOMO-4→LUMO	per
15	371	220→228	HOMO-6→LUMO+1	por+thio→por
		221→228	HOMO-5→LUMO+1	por+thio→por
		222→228	HOMO-4→LUMO+1	por
		222→229	HOMO-4→LUMO+2	por
		224→229	HOMO-2→LUMO+2	por+thio→por
		224→230	HOMO-2→LUMO+3	por+thio→thio
		225→229	HOMO-1→LUMO+2	por+thio→por
		225→230	HOMO-1→LUMO+3	por+thio→thio
		226→230	HOMO→LUMO+3	por+thio→thio
16	369	220→228	HOMO-6→LUMO+1	por+thio→por
		220→229	HOMO-6→LUMO+2	por+thio→por
		222→228	HOMO-4→LUMO+1	por
		222→229	HOMO-4→LUMO+2	por
		224→230	HOMO-2→LUMO+3	por+thio→thio
		225→230	HOMO-1→LUMO+3	por+thio→thio

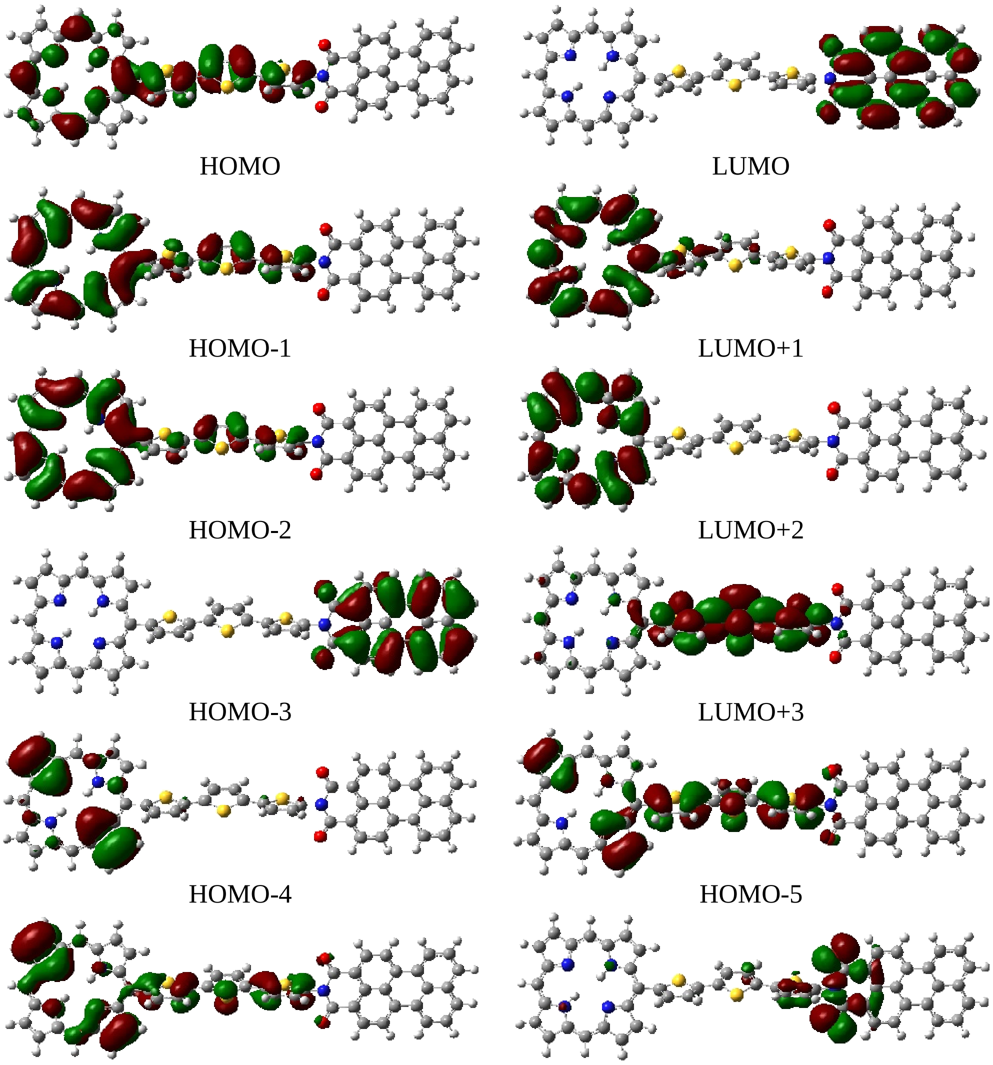

HOMO LUMO

HOMO-1 LUMO+1

HOMO-2 LUMO+2

HOMO-3 LUMO+3

HOMO-4 HOMO-5

HOMO-6 HOMO-10

Figure A.3 Visualized frontier molecular orbital for excitation of absorption spectra of Por-3Thio-Per compound.

APPENDIX B

Structural and electronic properties of porphyrin-thiophene-perylene compound as studied by quantum cemical calculations

Tatiya Chokbunpiam, Patchanita Thamyongkit, Oraphan Saengsawang
and Supot Hannongbua

13 th International annual symposium on computational science and engineering
(ANSCSE 13)

Structural and Electronic Properties of Porphyrin-Thiophene-Perylene Compound As Studied by Quantum Chemical Calculations

Tatiya Chokbunpiam[1,2], Patchanita Thamyongkit[3], Oraphan Saengsawang[2] and Supot Hannongbua [2,*]

[1]Petrochemical and Polymer Science Program, Faculty of Science, Chulalongkorn University, Bangkok 10330 Thailand
[2]Computational Chemistry Unit Cell (CCUC), Department of Chemistry, Faculty of Science, Chulalongkorn University,Bangkok 10330 Thailand
[3]Department of Chemistry, Faculty of Science, Chulalongkorn University, Bangkok 10330 Thailand
*supot.h@chula.ac.th

ABSTRCT

Dye-sensitized solar cells (DSC) have been attracted the interest of scientists because of its relatively high light-to-energy conversion, hence, they become one of the most promising alternative sources of energy. The π-conjugated system in organic dye compound has been known to absorb light and transform to energy via electron transfer. Porphyrin, a derivative of chlorophyll, is a good electron donor whereas perylene is widely used as an electron acceptor. The latter effectively adsorb visible light in the range 450-550 nm which is the region where porphyrin has relatively weak absorption. To extend the adsorption range of the light sensitizer, we designed a new compound consisting of porphyrin macrocycle linked to perylene unit via a thiophenic bridge, namely, Porphyrin-Thiophene-Perylene (Por-Thio-Per) compound. Structural and electronic properties of the proposed molecule were studied using the density functional theory at the B3LYP/6-31G(d) level. The results indicated that the electron transfer from porphyrin to perylene units through the thiophene linkage does not significantly affect the characteristic adsorption behavior of both chromophores and also demonstrated strong absorption peaks of Por-Thio-Per at 370-650 nm.

Keywords: Organic dye-sensitized solar cells, Porphyrin, Perylene, Thiophene

INTRODUCTION

Due to exhaustion of fossil fuels, renewable energy sources are of wide interest. Dye-sensitized solar cells (DSC) offer an interesting alternative to oil and gas by Gräzel and co-workers in 1954, uses a nanostructure semiconductor combined with dye molecules[1]. They have attracted attention of scientists from various fields because of photophysical, electrochemical properties, the variously modified structures and non toxic environment[2]. The dye molecules be responsible for the light absorption, the cell can be built from cheap and easily produced components such as porphyrin and perylene molecules to convert energy from sun to electricity passing through electron transfer. Porphyrin, a derivative of chlorophyll, is a good electron donor and can effectively adsorb visible light in the range 370-550 nm, whereas perylene is widely used as an electron acceptor and can effectively adsorb visible light in the range 450-550 nm[3]. Thiophene is often proposed in the literatures[4,5] to be used as the linker for electron transfer.

In this article, detailed photophysical of the free-base porphyrin and perylene connected with 2,5-thiophenic linker (Por-Thio-Per) compound as shown in Fig. 1c was examined. The structural, in term of conformation search, and electronic properties, in term of HOMO, LUMO as well as adsorption spectra of the Por-Thio-Per compound were investigated using quantum chemical calculations. In addition, excitation states and frontier molecular orbitals of the Por-Thio-Per compound were also analyzed.

2. COMPUTATIONAL METHOD

2.1 Optimal structure of the Porphyrin-Thiophene-Perylene compound

Initial structure of the Por-Thio-Per compound was created using GaussView program and shown in Fig. 1c. The following two conformational searches were, then, applied using the B3LYP with the 6-31gd basis set; *(i)* The torsion angle of the por-thio and per-thio (defined in Fig. 1c) was fully optimized while its geometries, bond lengths and bond angles, were kept constant throughout; and *(ii)* similar to *(i)* but the torsional angle was searched manually, *i.e.,* the first por-thio torsional angle (α_{Por}) was fixed at 0° while the per-thio torsional angle (α_{Per}) was scanned from 0° to 180° with the interval 30°. This procedure was, then, repeated by keeping the α_{Por} at 30°, 60°, 90°, 120°, 150° and 180°. In order to get higher accurate conformation, the two procedures, *(i)* and *(ii),* were, again, repeated in the range around the optimal α_{Por} and α_{Per} angles with the intervals 5° and 2°.

2.2 Electronic properties of Free-Base Porphyrin, Perylene, and *Porphyrin-Thiophene-Perylene compounds*

The calculations were focused to these three compounds, free base porphyrin, perylene and Por-Thio-Per compounds (Figs. 1a-1c). The optimal structures obtained from (2.1) were applied to calculate electronic excitation and the corresponding adsorption spectra using TD-B3LYP with 6-31G(d) basis set. All calculations were carried out using the Gaussian03 program package[6].

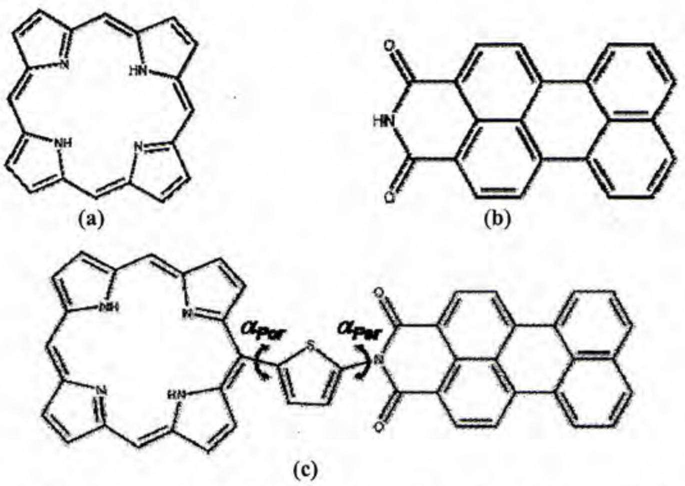

(a)

(b)

(c)

Figure 1 Chemical structures of (a) free base porphyrin, (b) perylene, and (c) Por-Thio-Per compounds.

3. Results and Discussion

3.1 Optimal Structure of Porphyrin-Thiophene-Perylene compound

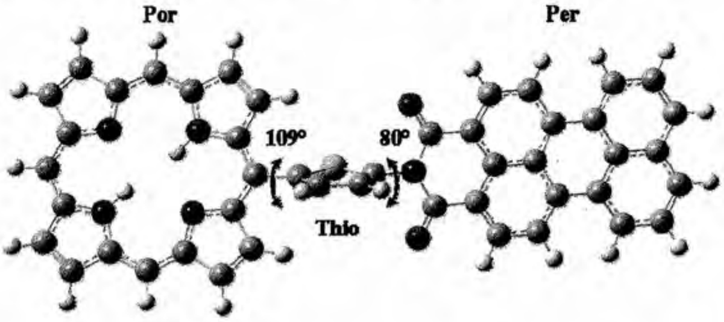

Figure 2 Optimal structure of the Por-Thio-Per compound where the obtained torsional angles were also shown.

Potential energy surface as a function of the two torsional angles obtained from the B3LYP/6-31g(d) optimization was shown in Fig. 3 in which the optimal α_{Por} and α_{Per} angles of 109° and 80° were, respectively, yielded.

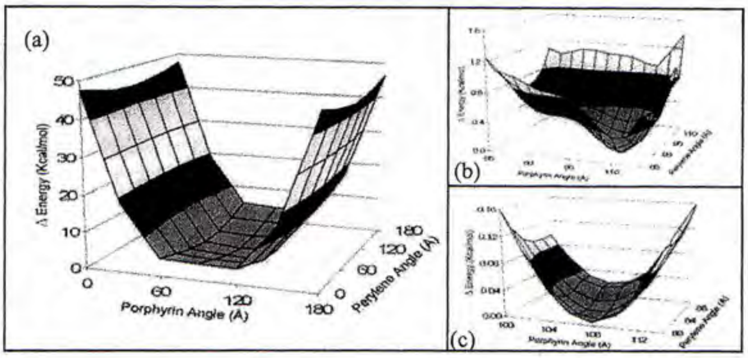

Figure 3 Potential energy surface obtained from the conformational search of the Por-Thio-Per compound varying (a) $-180^{\circ} \leq \alpha_{Por}, \alpha_{Per} \leq 180^{\circ}$, (b) $65^{\circ} \leq \alpha_{Por}, \alpha_{Per} \leq 110^{\circ}$, and (c) $100^{\circ} \leq \alpha_{Por} \leq 110^{\circ}$ and $80^{\circ} \leq \alpha_{Per} \leq 90^{\circ}$ with the intervals of 30°, 5° and 2°, respectively.

With the interval search of 30° where $-180^{\circ} \leq \alpha_{Por}, \alpha_{Per} \leq 180^{\circ}$, the optimal angles take place at $-120^{\circ} \leq \alpha_{Por}, \alpha_{Per} \leq 60^{\circ}$ (Fig. 3a). With a finer scale search, interval of 5°, the obtained results are $100^{\circ} \leq \alpha_{Por} \leq 110^{\circ}$ and $80^{\circ} \leq \alpha_{Per} \leq 90^{\circ}$. Finally, the search with $100^{\circ} \leq \alpha_{Por} \leq 110^{\circ}$ and $80^{\circ} \leq \alpha_{Per} \leq 90^{\circ}$ and the interval of 2° leads to the optimal α_{Por} and α_{Per} angles of 109° and 80° were, respectively. This conformation was, then, used to calculate the electronic properties of the compound.

3.2 Electronic properties of Free-Base Porphyrin, Perylene, and Porphyrin-Thiophene-Perylene compounds

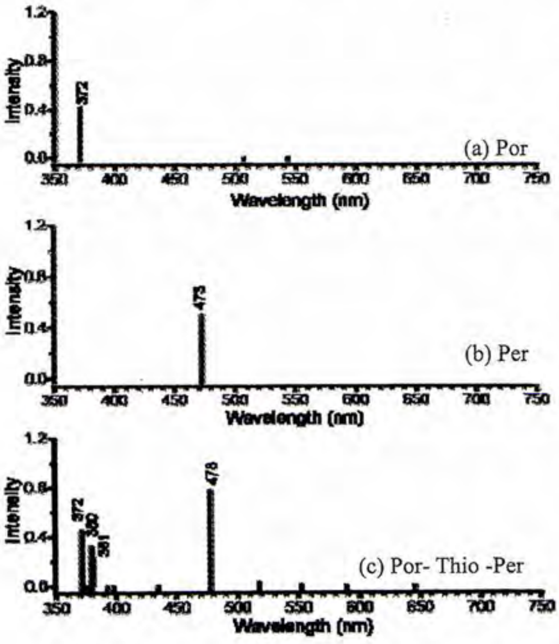

The plots of adsorption spectra for free-base porphyrin, perylene, and Por-Thio-Per compounds were shown in Figs. 4a, 4b, and 4c, respectively. The obtained peaks at 372 nm for the Por and 473 nm for the Per molecules are in good agreement with those yielded experimentally[7,8]. Several peaks were observed for the Por-Thio-Per compound in which interest was focused to the four high intensity peaks at 372, 380, 381 and 478 nm. The adsorption spectra at 372 and 478 nm which are the characters of the Por and Per molecules, respectively, remain unchanged. To understanding electronic properties and excitations of these four peaks, frontier molecular orbital were summarized in Table 1. The corresponding 10 frontier molecular orbitals were visualized in Fig. 5.

Figure 4 The absorption spectrum of the (a) Por, (b) Per, and (c) Por-Thio-Per compounds.

Table 1 Excited states of the adsorption spectra and the corresponding frontier molecular orbital of the Por-Thio-Per compound.

Excited state	Wavelength (nm)	Excitation	Frontier molecular orbital	Character of orbital
5	478	182→185	HOMO-2→LUMO	per
9,10	381,380	179→186	HOMO-5→LUMO+1	por
		179→187	HOMO-5→LUMO+2	por
		180→186	HOMO-4→LUMO+1	por
		180→187	HOMO-4→LUMO+2	por
		182→187	HOMO-2→LUMO+2	per → por
		183→186	HOMO-1→LUMO+1	por
		183→187	HOMO-1→LUMO+2	por
		184→186	HOMO→LUMO+1	por
		184→187	HOMO→LUMO+2	por
12	372	179→186	HOMO-5→LUMO+1	por
		179→187	HOMO-5→LUMO+2	por
		181→186	HOMO-3→LUMO+1	thio→ por
		183→186	HOMO-1→LUMO+1	por
		183→187	HOMO-1→LUMO+2	por
		184→186	HOMO→LUMO+1	por
		184→187	HOMO→LUMO+2	por

In Table 1, the frontier molecular orbital which corresponds to each excitation was characterized. According to the visualization shown in Fig. 5, the frontier molecular orbitals were categorized by the position of electron density cloud into three groups; *(i)* HOMO, HOMO-1, HOMO-4, HOMO-5, LUMO+1, LUMO+2, *(ii)* LUMO, HOMO-2 and *(iii)* HOMO-3, HOMO-6. The three groups *(i)-(iii)* yield from porphyrin unit, perylene unit and thiophene bridge, respectively.

In terms of electron transfers, the HOMO-LUMO excitations can be classified into two types where the excitation was generated from the same and from different molecular units in the Por-Thio-Per compound, known as "specific" and "crossing" excitations, respectively. Excited state number 5 (Table 1) indicates specific excitation corresponding to the perylene spectrum at 478 nm. In addition, state numbers 9, 10 and 12 are combined specific excitation of porphyrin and crossing excitation between perylene to porphyrin (per→por) as well as thiophene to porphyrin (thio→por).

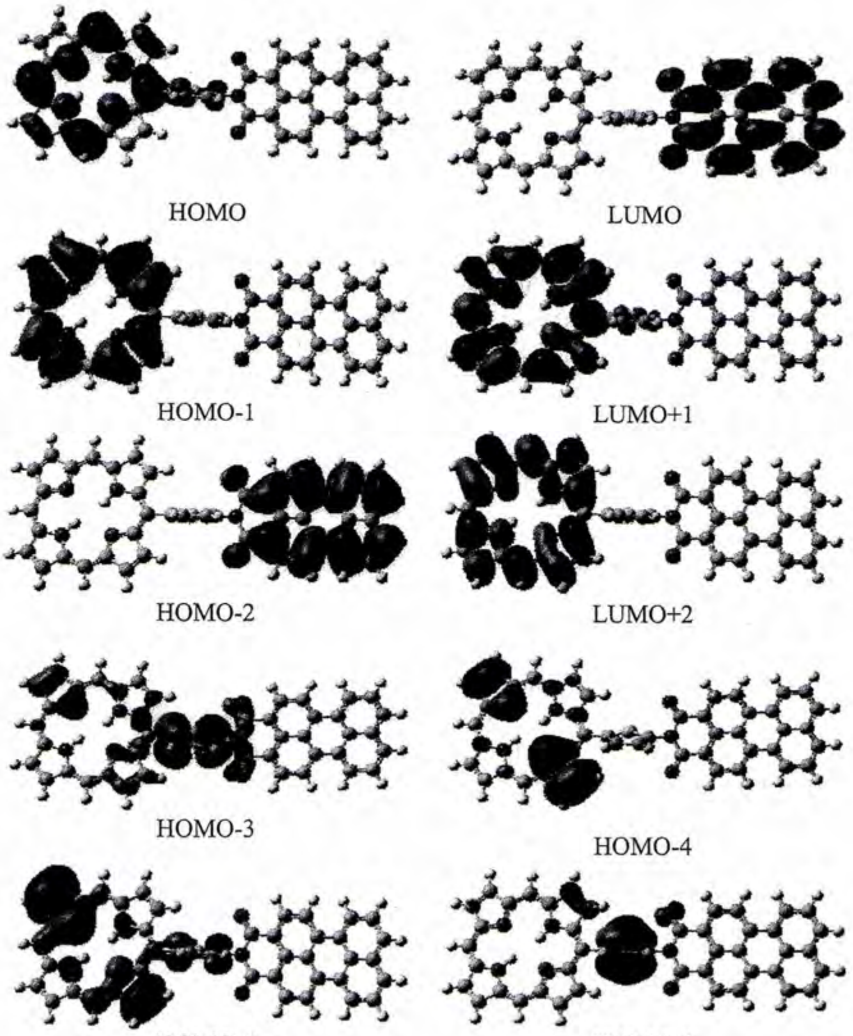

HOMO LUMO

HOMO-1 LUMO+1

HOMO-2 LUMO+2

HOMO-3 HOMO-4

HOMO-5 HOMO-6

Figure 5 Visualized frontier molecular orbital for the excited adsorption spectra of Por-Thio-Per compound.

4. Conclusions

The B3LYP/6-31G(d) level of accuracy is the optimal method compromising between accuracy and computational cost for fully optimization and conformation searching of the calculated system. Por-Thio-Per compound generates strong adsorption spectra at 478, 381, 380 and 372 nm and enhances the spectra such in the range 370-650 nm. Moreover, characteristic of perylene at 478 nm and of porphyrin unit 377 nm does not affect from the Por-Thio-Per compound.

LITERATURE CITED

1. M. Gräzel, *J. Photochem. Photobiol.A*, 2004, **164**, 3-14.
2. H. Hoppe and N. S. Sariciftci, *J. Mater. Res.*, 2004, **19**(7), pp. 1924-1944.
3. S. Prathapan, S. I. Yang, J. Seth, M. A. Miller, D. F. Bocian, D. Holten, and J. S. Lindsey, *J. Phys. Chem. B*, 2001, **105**, pp. 8237-8248.
4. H. Choi, J. K. Lee, K. Song, S. O. Kang, and J. Ko, *Tetrahedron*, 2007, **63**, pp. 3115-3121.

5. S. Kim, H. Choi, K. Song, S. O. Kang, and J. Ko, *Tetrahedron*, 2007, **63**, pp.11436-11443.
6. M. J. Frisch, G. W. Trucks, H. B. Schlegel, G. E. Scuseria, M. A. Robb, J. R. Cheeseman, J. Montgomery, J. A., T. Vreven, K. N. Kudin, J. C. Burant, J. M. Millam, S. S. Iyengar, J. Tomasi, V. Barone, B. Mennucci, M. Cossi, G. Scalmani, N. Rega, G. A. Petersson, H. Nakatsuji, M. Hada, M. Ehara, K. Toyota, R. Fukuda, J. Hasegawa, M. Ishida, T. Nakajima, Y. Honda, O. Kitao, H. akai, M. L. Klene, X., J. E. Knox, H. P. Hratchian, J. B. Cross, V. Bakken, C. Adamo, J. Jaramillo, R. Gomperts, R. E. Stratmann, O. Yazyev, A. J. Austin, R. Cammi, C. Pomelli, J. W. Ochterski, P. Y. Ayala, K. Morokuma, G. A. Voth, P. Salvador, J. J. Dannenberg, V. G. Zakrzewski, S. Dapprich, A. D. Daniels, M. C. Strain, O. Farkas, D. K. Malick, A. D. Rabuck, K. Raghavachari, J. B. Foresman, J. V. Ortiz, Q. Cui, A. G. Baboul, S. Clifford, J. Cioslowski, B. B. Stefanov, G. Liu, A. Liashenko, P. Piskorz, I. Komaromi, R. L. Martin, D. J. Fox, T. Keith, M. A. Al-Laham, C. Y. Peng, A. Nanayakkara, M. Challacombe, P. M. W. Gill, B. Johnson, W. Chen, M. W. Wong, C. Gonzalez, J. A. Pople, Gaussian, Inc., Wallingford CT, 2004
7. D. Sundholm, *Phys. Chem. Phys.*, 2000, **2**, pp. 2275-2281.
8. S. I. Yang, R. K. Lammi, S. Prathapan, M. A. Miller, D. F. Bocian, J. S. Lindsey, and D. Holten, *J. Material Chemisty*, *2001*, **11**, *pp.2420-2430.*

ACKNOWLEDGMENTS

Financial supporting from the Thailand research fund-master research grants-window II (TRF-MRG-WII Project 515S045) and National center of excellence for petroleum, petrochemicals, and advanced materials (NCE-PPAM) are gratefully acknowledged. All facilities and computer resources are provided by the Computational Chemistry Unit Cell at Department of Chemistry, Faculty of Science, Chulalongkorn University.

APPENDIX C

MANUSCRIPT

Molecular Structure and Electronic Properties of Porphyrin-Thiophene Perylene using Quantum Chemical Calculation

Tatiya Chokbunpiam, Patchanita Thamyongkit, Oraphan Saengsawang
and Supot Hannongbua

To be submitted

Molecular Structure and Electronic Properties of Porphyrin-Thiophene Perylene using Quantum Chemical Calculation

Tatiya Chokbunpiam[1,2], Patchanita Thamyongkit[3], Oraphan Saengsawang[2] and Supot Hannongbua[2*]

[1] *Petrochemical and Polymer Science Program, Faculty of Science, Chulalongkorn University, Bangkok 10330 Thailand*
[2] *Computational Chemistry Unit Cell (CCUC), Department of Chemistry, Faculty of Science, Chulalongkorn University,Bangkok 10330 Thailand*
[3] *Department of Chemistry, Faculty of Science, Chulalongkorn University, Bangkok 10330 Thailand*

Abstract

The main propose of this study aims to design a new series of compounds consisting of porphyrin (Por) macrocycle linked to perylene (Per) unit via a thiophenic bridge. Structural and electronic properties of the molecules, as well as the effect of mono- and bi-substituents R on C3 and R′ on C4 of thiophene ring were studied using quantum calculation approach. The method used was validated and found that the B3LYP/6-31G(d) is the optimal one compromising between the accuracy and the computer time required. The results indicated that significant changes of the torsion angle between the molecular planes of the Por and Per rings were found only for the two bi-substituted derivatives, R = R′ = $–OCH_3$ and $–NH_2$, and one mono-substituted derivative, R = –H and R′ = $–NH_2$. These can be clearly described in terms of interaction between the substituted groups and one or both oxygen atoms of the Per unit. The symmetric bi-substituent does not provide significantly lower of the HOMO-LUMO energy gap (ΔE_g). Noticeable decrases of the ΔE_g were found only when the substituents are the electron donor groups, taken place only for the four newly designed derivatives where R,R′ = $–OCH_3$,H; –OH,H; $–N(CH_3\ )_2$,H and –H,NH_2 with the reduction of the ΔE_g by -0.157 eV, -0.157 eV, -0.118 eV and -0.134 eV, respectively. It was also found that the UV-visible spectra of the derivatives cover a broader range, 370-730 nm, compared to those between 450 nm and 550 nm for the two free bases Por and Per and characteristics of the Por and Per molecules, which indicate by the absorptions spectra at 372 and 473 nm, remain unchanged.

Keywords: organic dye-sensitized solar cells, porphyrin, perylene, thiophene, quantum chemical calculation

---

* To whom correspondence should be sent

E-mail address: supot.h@chula.ac.th (Supot Hannongbua)

1. Introductions

Since the present cost of electricity from silicon-based photovoltaics (PVs) is much higher than the current commercial prices of electricity generated by hydraulic power and nuclear and fossil fuels. Therefore, it is necessary to develop low-cost solar cells with high power conversion efficiency. As promising candidates to fulfill these requirements, organic-based solar cells have attracted attention of scientists. One of the key developments of organic compounds for dye-sensitized solar cells comes from the molecular design in order to tune photophysical, electrochemical and optical properties of the molecules. This becomes the main propose of this study which focus to design a new series of compounds consisting of porphyrin macrocycle linked to perylene unit via a thiophenic bridge that exhibiting an extended absorption range, narrow band gap and potential electronic transfer by using quantum chemical calculation.

After the firstly pioneered fabrication of dye-sensitized solar cells (DSC) by Gräzel in 1954,[1] solar cell researchers have put their best effort to understand device function in order to achieve the improvement of light harvesting efficiency and feasibility of the device for commercial purposes. Photosynthetic pigments related to the chlorophylls, such as porphyrins, are particularly promising light absorbers for solar cell applications, owing to their large molar absorption coefficients, tunable photophysical properties, and amenability to molecular modification. Porphyrin is a good electron donor and can effectively adsorb in the near-UV region which, however, is a rather small fraction of solar photons. One of the most promising approaches for the molecular design of organic light-harvesters is utilizing structurally related chromophores that absorb strongly in the trough between the porphyrin Soret (B) and Q-bands. Highly suitable chromophores for this requirement and that is taken into the consideration in this study are perylene compounds. The use of perylene as accessory pigment in the porphyrin system was found attractive for light-harvesting application as high near-infrared absorption coefficient, rapid and efficient energy transfer, and satisfactorily long lifetime of the resulting molecules were provided.[2,3]

Since well understanding of electronic properties such as energy gap, and HOMO and LUMO levels, is a key factor to design new and appropriate structure of organic dye compound and, hence, to increase efficiency in solar cell applications, the goal of this work is to theoretically predict such structural and electronic properties of a novel porphyrin-perylene dyad bridged by 2,5-thiophenylene linker using quantum chemical calculation. Incorporation of the thiophene moiety in several previously studied binuclear systems afforded effective intermolecular electronic communication.[4] In this work, we firstly focused on the structural optimization in term of the intermolecular torsion angle using a simple B3LYP/6-31G(d) method. After that, the calculation outcome in terms of HOMO and LUMO levels, energy gap, and CPU time resulted from the same method with different size of basis sets were compared to seek for the method of choice for further studies concerning effect of various substituents at 3- and/or 4-position of the thiophene linker on structural and electronic properties and computational investigation of absorption spectra of these derivatives. The approach is general and could be useful for studying other systems containing other organic light-sensitizers.

2. Computational methods

2.1 Optimal structure of Porphyrin-Thiophene-Perylene sensitizer compound

The initial structure of the Por-Thio-Per compound, where R=R' =H, was generated using GaussView program and shown in Figure 1. As it is successfully used in the previous studies[5-12], the density functional theory (DFT) approach at the B3LYP with the 6-31G(d) basis set was used in this study to search for the optimal structure of the investigated compound. Here, two procedures were separately applied, (*i*) the structure was fully optimized, *i.e.*, all atoms were allowed to relax. *(ii)* to examine whether the obtained structure is the global minimum energy conformation, two torsion angles, θ and ϕ, shown in Figure 1 were defined. Then, its geometries, bond lengths and bond angles obtained from (*i*), were kept constant throughout, whereas, the torsion angles were optimized using the following manner. The angle θ was fixed at 0˚ while ϕ was scanned from 0˚ to 180˚ with the interval 30˚. This procedure was, then, repeated by keeping θ at 30˚, 60˚, 90˚, 120˚, 150˚ and 180˚. In order to get more precise conformation, the procedures *(ii)* was, again, repeated in the range around the optimal θ and ϕ angles with the intervals 5^o and 2^o. All calculations were performed using the Gaussian03 program package[13].

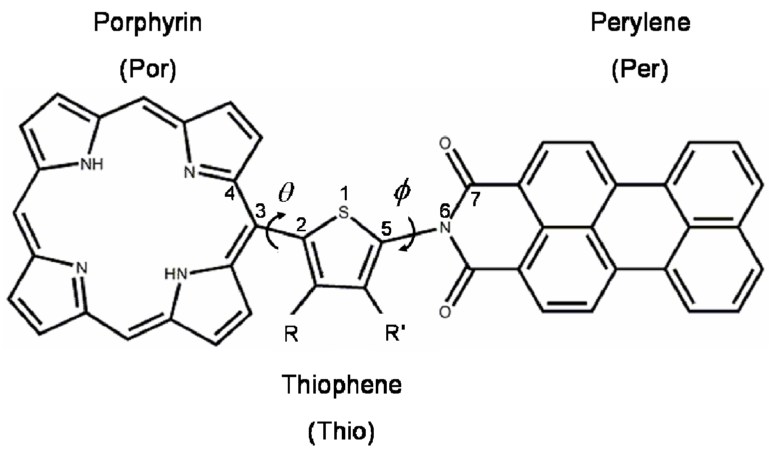

Figure 1 Two-dimensional structure of the Por-Thio-Per sensitizer compound (R = R′ = –H) and its derivatives where *(i)* R = –H, R′ = –H, $-CH_3$, $-OCH_3$, –OH, $-NH_2$, $-N(CH_3)_2$, –CN and $-NO_2$ *(ii)* R = –H, $-CH_3$, $-OCH_3$ –OH, $-NH_2$, $-N(CH_3)_2$, –CN and $-NO_2$, R′ = –H, *(iii)* R = R′ = –H, $-CH_3$, $-OCH_3$ –OH, $-NH_2$, $-N(CH_3)_2$, –CN and $-NO_2$. The torsion angles, θ and ϕ, were defined by 1-2-3-4 and 1-5-6-7, respectively.

2.2 Optimal structure of Porphyrin-Thiophene-Perylene derivatives

Interest was focused to the derivatives with the following electron donating ($-CH_3$, $-OCH_3$ –OH, $-NH_2$ and $-N(CH_3)_2$) and the electron withdrawing (–CN and $-NO_2$) groups. Starting from the optimal structure of the Por-Thio-Per compound where R = R′ = H, the following derivatives were built, *(i)* R = –H, R′ = $-CH_3$, $-OCH_3$ –OH, $-NH_2$, $-N(CH_3)_2$, –CN and $-NO_2$ *(ii)* R = $-CH_3$, $-OCH_3$ –OH, $-NH_2$, $-N(CH_3)_2$, –CN and $-NO_2$, R′ = H, *(iii)* R = R′ = $-CH_3$, $-OCH_3$ –OH, $-NH_2$, $-N(CH_3)_2$, –CN and $-NO_2$. Note that, the derivatives where $R \neq R'$ are not taken into account to simplify the data interpretation in the first place and, in addition, it is because asymmetric substitution on thiophene ring is synthetically complicated. To search for the most stable structure of these compounds, two steps of partial optimization were subsequently applied. First, only geometries of the substituted groups (while those of the other atoms were taken from 2.1 and kept constant throughout) were fully optimized. Then, the obtained geometry were fixed and the two torsion angles (θ and ϕ) were adjusted in order to seek for the preferential conformation of the derivatives.

2.3 Optimal method for the electronic property investigations

With the optimal structure of the Por-Thio-Per compound and its derivatives obtained from 2.1 and 2.2, the B3LYP calculations at different basis sets: 6-31G(d), 6-31G(d,p), 6-31G+(d) and 6-31G+(d,p) have been performed. Seeking for compromising between the accuracy and the required computer time, the electronic properties of the calculated systems were used to validate the method applied. The resulting optimal method was, then, used for the investigation of the electronic properties of the molecule of interest throughout.

3. Results and Discussions

3.1 Optimal structure of Porphyrin-Thiophene-Perylene sentsitizer compound

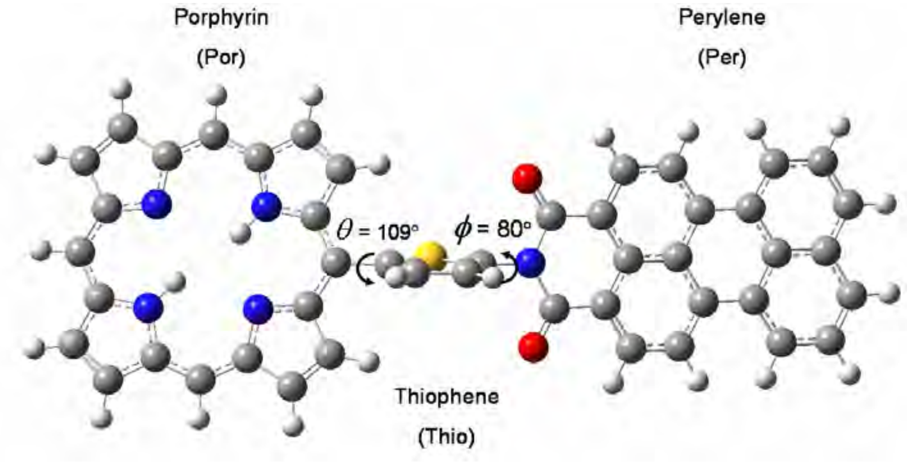

Figure 2 The optimal structure of the Por-Thio-Per compound (R = R′ = H) where θ = 109° and ϕ = 80°, obtained from the B3LYP/6-31G(d) calculation.

With the fully optimization procedure and the B3LYP/6-31G(d) method, the calculated structure of the Por-Thio-Per compound where R = R′ = –H takes place at the torsion angles θ and ϕ of 109° and 80°, respectively (Figure 2). In another approach, the potential energy surfaces, where θ and ϕ were optimized manually at the angle intervals 30^o, 5^o and 2^o, were shown in Figures 3a, 3b and 3c, respectively. As shown in Figure 3c, the calculated energy minimum lies in the ranges 106°-110°

for θ and 80°-84° for ϕ. Good agreement between the results yielded from the two optimized procedures indicates reliability of the obtained structure.

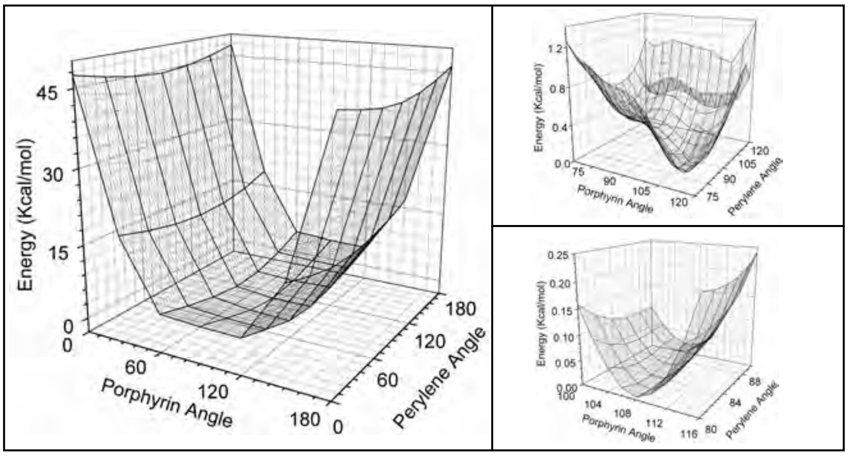

Figure 3 (a)-(c) potential energy surfaces of the Por-Thio-Per sensitizer compound, where R = R′ = –H, as a function of the torsion angles (θ and ϕ defined in Figure 2) optimized manually at the angle intervals 30^{o}, 5^{o} and 2^{o}, respectively.

3.2 Optimal method for the electronic properties investigations

With the optimal configuration of the Por-Thio-Per (R = R′ = –H) compound where θ = 109° and ϕ = 80°, the B3LYP method at different sizes of the basis sets were applied to examine electronic properties of the investigated compound. This procedure was taken into account in order to seek for the optimal level of accuracy, compromising between reliability of the calculated results and the CPU (Computation Processing Units) time needed. The HOMO, LUMO and energy gap as well as the required CPU times were summarized in Table 1. Examinations were also extended to the Por-Thio-Per and its derivatives where R = R′ = –OCH_3, –OH, –CN and –NO_2. The results were compared in Figure 4.

As clearly seen from Table 1, significant differences of the HOMO and LUMO energies were yielded when the diffusion function, 6-31G+(d) and 6-31G+(d,p) were included. As expected, the absolute energies were found not to effect the HOMO-LUMO energy band gap significantly, -2.1619 eV, -2.1608 eV, -2.1149 eV and -2.1143 eV for the 6-31G(d) and 6-31G(d,p), 6-31G+(d) and 6-31G+(d,p) bassis sets, respectively. These conclusions were also true for the selected Por-Thio-Per derivatives where the energy data were shown in Figure 4. Since the same level of accuracy has to be applied for all four defined in Figure 1 and the CPU time required to take into account the diffusion functions (6-31G+(d) and 6-31G+(d,p)) is dramatically higher than those of the other two basis sets, therefore, the B3LYP with the 6-31G(d) was chosen to be the optimal method for the electronic properties calculations for all compounds in this study.

Table 1 HOMO, LUMO, energy gap and CPU times yielded from the B3LYP method at different sizes of the basis sets for the Por-Thio-Per where R = R′ = –H, θ = 109° and ϕ = 80° (see Figure 2 for definition).

Method	HOMO (eV)	LUMO (eV)	Energy Gap (eV)	CPU time (hr:min)
B3LYP/6-31 G(d)	-5.030	-2.868	2.162	0:44
B3LYP/6-31 G(d,p)	-5.040	-2.880	2.160	0:51
B3LYP/6-31+ G(d)	-5.323	-3.208	2.115	9 :42
B3LYP/6-31+ G(d,p)	-5.334	-3.220	2.114	10:12

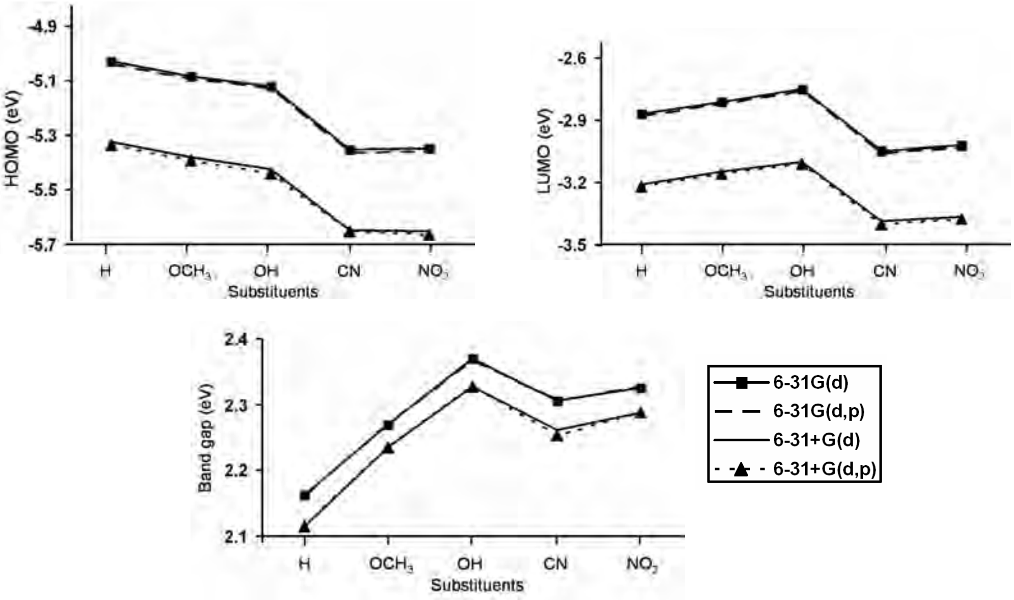

Figure 4 (a) HOMO, (b) LUMO and (c) energy gap of the Por-Thio-Per compound (where R = R′ = –H) and its derivatives (where R = R′ = –H, –OCH_3, –OH, –CN and –NO_2) calculated using the B3LYP method with different basis sets.

With the selected B3LYP 6-31G(d) calculation, the frontier molecular orbitals corresponding to the HOMO and LUMO energies for the most stable structure of the Por-Thio-Per compound where R = R′ = –H were visualized and shown in Figure 5. The HOMO energy was mapped to the porphyrin unit whereas the LUMO one was found to locate on the perylene unit, *i.e.*, the porphyrin and the perylene were assigned to act as the electron donor and electron acceptor, respectively. From the plots, electron transfer from porphyrin to perylene, which is the important feature for the electronic conductivity in solar cell application was clearly visualized.

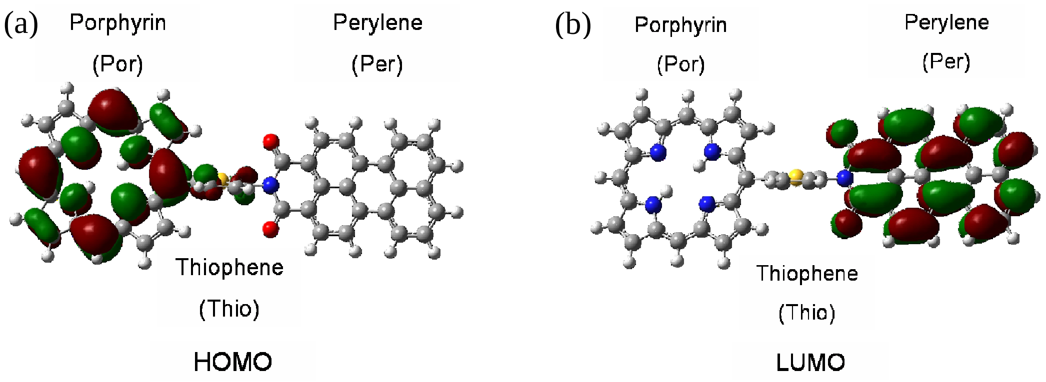

Figure 5 Frontier molecular orbital of (a) HOMO and (b) LUMO visualized by TD-B3LYP 6-31G(d) calculations indicated the electron donor and electron acceptor features of the porphyrin and perylene units, respectively.

3.3 Structure and electronic property of the Por-Thio-Per derivatives

Table 2 Changes of the torsion angles ($\Delta\theta$ and $\Delta\phi$ defined in Figure 2) and the corresponding energy gap (ΔE_g) of the Por-Thio-Per derivatives obtained from the B3LYP 6-31G(d) calculations relative to those of the Por-Thio-Per compound (R = R′ = –H), subtract the values obtained from the Por-Thio-Per compounds by those of its derivatives.

Substituent	Torsion angle (degree)			ΔE_g (eV)
R/R′	$\Delta\theta$	$\Delta\phi$	$\lvert\Delta\phi\text{-}\Delta\theta\rvert$	
Bi-substituent				
H,H	0.0	0.0	0.0	0.0
CH_3,CH_3	-7	4	11	0.019
OCH_3,OCH_3	-2	**20**	**22**	0.108
OH,OH	5	5	0	0.209
NH_2,NH_2	4	**-19**	**23**	-0.089
$N(CH_3)_2$, $N(CH_3)_2$	-1	8	9	-0.086
CN,CN	0	0	0	0.143
NO_2,NO_2	-7	6	13	0.164
Mono-substituent				
CH_3,H/H,CH_3	-6/4	3/-7	9/11	0.045/-0.051
OCH_3,H/H,OCH_3	0/2	1/5	1/3	**-0.157**/0.097
OH,H/H,OH	-1/0	0/0	1/0	**-0.157**/0.128
NH_2,H/**H,NH_2**	1/5	1/**-16**	0/**21**	-0.065/**-0.134**
$N(CH_3)_2$,H/H, $N(CH_3)_2$	2/3	6/3	4/0	**-0.118**/0.028
CN,H/H,CN	-3/0	-1/1	2/1	0.016/0.143
NO_2,H/H,NO_2	-3/2	1/4	4/2	-0.022/0.205

Referred to the calculation details given in 2.2, changes of the torsion angles ($\Delta\theta$ and $\Delta\phi$ defined in Figure 2) and the corresponding energy gap (ΔE_g) of the Por-Thio-Per derivatives obtained from the B3LYP 6-31G(d) calculations relative to those of the Por-Thio-Per compound (R = R′ = –H) were extracted and summarized in Table 2. Here, the values obtained from the Por-Thio-Per compounds were subtracted by those of its derivatives. Therefore, negative value of the change of torsion angle denotes the rotation in the direction opposite to the arrow defined in Figure 2 whereas negative ΔE_g means that the newly designed derivative gives narrower energy gap and *vice* versa. In addition, absolute value of the $|\Delta\phi$-$\Delta\theta\ |$ implies the changes of the torsion angle between the two molecular planes of the porphyrin and perylene units.

In term of molecular structure, it is clearly seen from Table 2 that significant change of the torsion angle was found only for the two bi-substituted derivatives, R = R′ = –OCH_3 and –NH_2, and one mono-substituted derivative, R = –H and R′ = –NH_2 in which change of an angle between the porphyrin and perylene molecular planes ($|\Delta\phi$-$\Delta\theta\ |$) of >20^o (marked as bold characters in Table 2) was taken place. These findings can be described in terms of interaction between the substituted groups and one or both oxygen atoms of the perylene unit. Steric hindrance due to the –OCH_3 substituent repulses the oxygen atom of the perylene, leading to the positive $\Delta\phi$ (perylene was rotated in the direction of the arrow shown in Figure 1) by 20^o. This is not the case for the bi-substituted –$N(CH_3)_2$ in which repulsion between the this bulky group and the two oxygen atoms of perylene (see also Figure 1) was observed to tilt the angle ϕ by only 8^o. For the –NH_2, the perylene unit was rotated by -19^o for the bi-substituted and -16^o for the mono-substituted due to a weak intramolecular hydrogen bond with one of the hydrogen atom of perylene. This hydrogen bond could not be formed for the OH functional group because of the OH…O repulsion.

Interest was focused to the reduction of the HOMO-LUMO energy gap where the calculation results lead to the following conclusions. *(i)* The symmetric bi-substituent does not provide significantly lower of the ΔE_g, slightly narrower of the energy gaps of -0.089 eV and -0.086 eV were, however, observed for the derivatives where R = R′ = –NH_2 and –$(NCH_3\ )_2$, respectively. *(ii)* Noticeable changes of the HOMO-LUMO band gap were found for the four newly designed derivatives where R,R′ = –OCH_3,H; –OH,H; –$NCH_3\ )_2$,H and –H,NH_2 with the reduction of the ΔE_g by -0.157 eV, -0.157 eV, -0.118 eV and -0.134 eV, respectively. *(iii)* Decrease of the ΔE_g

was significantly observed only when the substituents are electron donor groups. However, no relation was found between degree of electron donation and the ΔE_g reduction. *(iv)* Among the four highly potential candidates, three substitutions were found to take place at the porphyrine unit, R,R′ = $–OCH_3$,H; –OH,H and $–NCH_3)_2$,H.

As concluded in *(iii)* and *(iv)*, substitution of the electron donor group to the porphyrine unit was observed to be the favorable choice for the design of the new compounds for the dye-sensitized solar cells. This finding can be clearly understood by the frontier molecular orbital shown in Figure 5 where the porphyrin unit was shown to serve as the electron donor. Therefore, increase of the electron density at this unit, due to the electron donor substituents, can directly facilitate the electron transfer to the perylene which is know to be a key factor for the dye-sensitized solar cells. However, this is not the case for what found for the mono-substituted $–NH_2$ at the perylene unit (R = –H and R′ = $–NH_2$) which lead also to decrease the energy gap by -0.134 eV (Table 2). The reason for this fact is due to the intramolecular hydrogen bond, which lead also to the change of the angle ϕ by -16^o as described above. This newly formed hydrogen bond was, then, assist the electron transfer to the perylene unit.

3.4 UV-visible spectra of the Por-Thio-Per derivatives

Using the TD-B3LYP calculations in the Gaussion03 package, the UV-visible spectra for the investigated compounds were calculates. The obtained results for the free-base porphyrin, the free-base perylene, the Por-Thio-Per compound and the four newly designed derivatives were summarized in Figure 6.

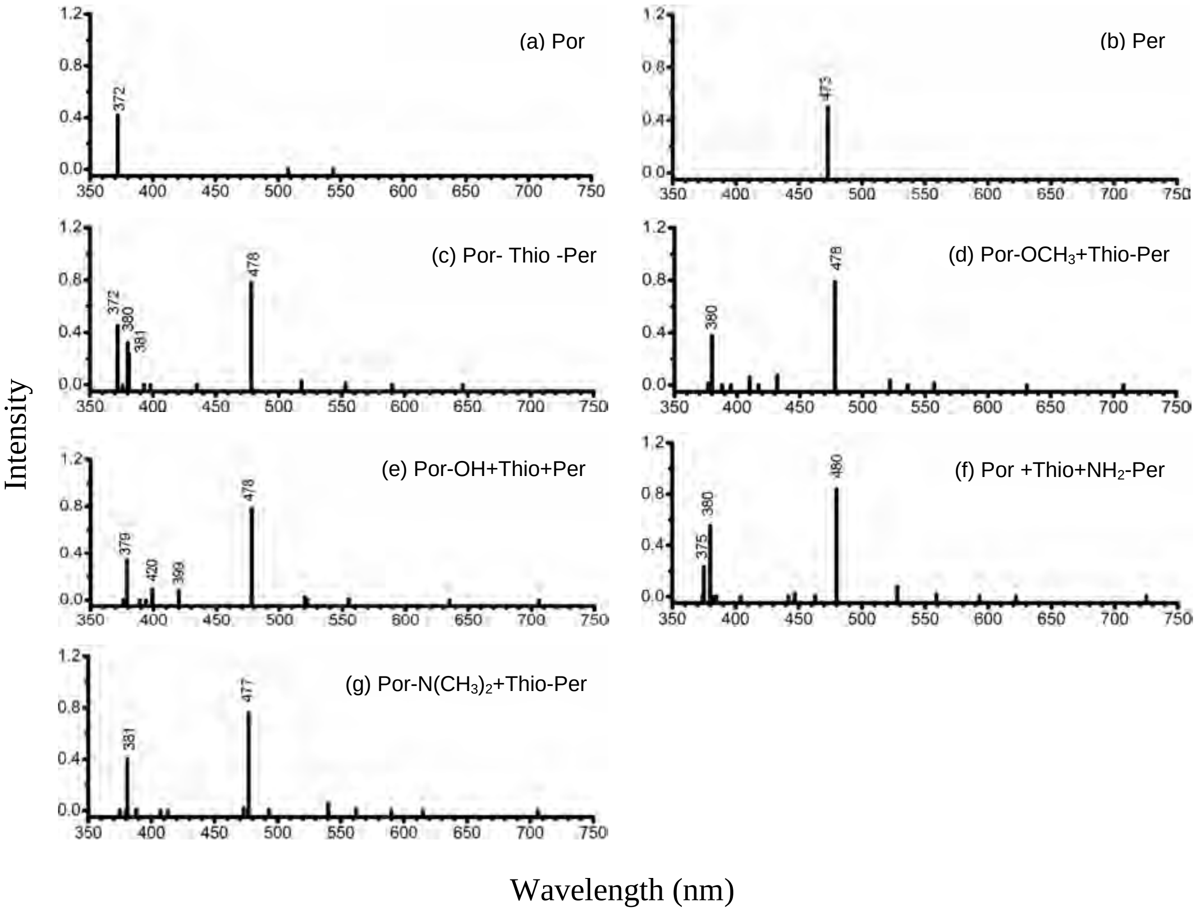

Figure 6 UV-visible spectra of the free base porphyrin, perylene, Por-Thio-Per compound (R = R´ = –H) and the four newly designed derivatives which provide significantly lower energy gap, relative to those of the Por-Thio-Per compounds (marked as bold characters in Table 2).

The free-base porphyrin shows maximum absorption spectra at 372 nm whereas the values for the perylene maximum at 473 nm (Figures 6a and 6b, respectively). The two calculated maxima, 372 and 473 nm, are in agreement with those yielded experimentally for the free-base porphyrin and perylene, respectively[14,15,16].

Several peaks were observed for the Por-Thio-Per compound (R = R´ = –H) and the four newly designed derivatives. It appears also that the absorption spectra of the Por-Thio-Per and its derivatives cover a broader range, 370-730 nm (Figures 6c-6g), compared to those between 372 nm and 473 nm for the two free bases (Figures 6a and 6b). The most important feature is that characteristics of the porphyrin and perylene molecules, which indicate by the absorptions spectra at 372 and 473 nm, remain unchanged. The first peak was only slightly shifted to 380 nm, 379 nm, 380 nm and 381 nm for the four derivatives, R = R´ = $–OCH_3$,H; –OH,H; –H,NH_2 and –$N(CH_3)_2$,H, respectively. The corresponding values for the second peaks of those derivatives are 478 nm, 478 nm, 480 nm and 477 nm.

4. Conclusion

This study focused on the investigation of structural] electronic and optical properties of a newly designed series of conjugated molecules bearing unsubstituted porphyrin and perylene linked via thiophenylene bridge. The thiophenylene bridge was assigned to be unsubstituted, monosubstituted or disubstituted. B3LYP/6-31G(d) level is the calculation method of choice serving as a compromising tool to accomplish the study with satisfactorily acceptable accuracy and computational cost. By this method, the optimum torsion angle between the molecular planes of the lateral porphyrin or perylene unit and the central thiophene ring, and the effect of substitution at 3- and/or 4-positions of the thiophene ring were intensively investigated. The results showed that the existence of the substituents predominantly affected the distortion of the torsion angle between the perylene and thiophene molecular planes, compared to that between the porphyrin and thiophene ones. Furthermore, energy band gaps and HOMO-LUMO energy levels of the molecules were both electronically and sterically influenced by types and position of the substituents. As regards excitation profiles, shift of the molecular electron density from porphyrin to perylene moieties in Por-Thio-Per model compound was observed, indicating the possible excited-state electronic communication in the molecule, which is a key mechanism in light-harvesting system. Moreover, predicted absorption of these compounds appeared to cover a range of 370-730 nm, wherein the beneficial characteristic absorption of porphyrin and perylene remain intact. These results suggested that Por-Thio-Per and its derivatives should be potential candidates for light-harvesting application. Detailed studies are in progress and will be published elsewhere.

5. References

1. M. Gräzel, *J. Photochem. Photobiol.A*, **2004**, *164*, 3–14.
2. Prathapan, S.; Yang, S. I.; Seth, J.; Miller, M. A.; Bocian, D. F.; Holten, D.; Lindsey, J. S. *J. Phys. Chem. B* **2001**, *105*, 8237–8248.
3. O’Neil, M. P.; Niemczyk, M. P.; Svec, W. A.; Gosztola, D.; Gaines, G. L., III; Wasielewski, M. R. *Science* **1992**, *257*, 63-65.
4. Selected publications: (a) Benniston, A. C.; Harriman, A.; Lawrie D. J.; Mayeux A. *Phys. Chem. Chem. Phys.* **2004**, *6*, 51–57. (b) Benniston, A. C.; Harriman, A.; Lawrie D. J.; Mayeux A.; Rafferty K.; Russell, O. D. *Dalton Trans.* **2003**, 4762–4269. (c) Hoshino, Y.; Suzuki T.; Umeda H. *Inorganica Chimica Acta.* **1996**, *245*, 87–90.
5. Yoshishige, O.; Toshiya, K.; Shiyoshi, Y.; Shinro, M., *Theochem*, **2002**, 55-60.
6. Yoshishige, O.; Toshiya, K.; Shiyoshi, Y.; Shinro, M., *Theochem*, **2003**, 631, 13-20.
7. Earles, C. J.; Gordon, C. K.; Officer, L. D.; Wagner, P., *J. Phys. Chem. A*, 111 (30), **2007**, 7171-7180.
8. Estrada, A. L.; Montes, A. V.; Zyryanov, G.; Anzenbacher, P., *J. Phys. Chem. B*, 111 (25), **2007**, 6983-6986.
9. Chen, Y.; Lin, Y.; EI-Khouly, E. M.; Zhuang, X.; Araki, Y.; Ito, O.; Zhang, W.; *J. Phys. Chem. C*, 111 (44), **2007**, 16096 -16099.
10. Hagberg, P. D.; Edvinsson, T.; Marinado, T.; Boschloo, G.; Hagfeldt, A.; Sun, L., *Chem. Commun*, **2006**, 2245–2247.
11. Petsalakis, D. I.; Tagmatarchis, N.; Theodorakopoulos, G., *J. Phys. Chem. C*, **2007**, 111, 14139-14149.
12. Zhang, X.; Zhang, J.; Xia, Y., *J. Photochem. Photobiol. A*, **2008**, 194, 167-172.

13. M. J. Frisch, G. W. Trucks, H. B. Schlegel, G. E. Scuseria, M. A. Robb, J. R. Cheeseman, J. Montgomery, J. A., T. Vreven, K. N. Kudin, J. C. Burant, J. M. Millam, S. S. Iyengar, J. Tomasi, V. Barone, B. Mennucci, M. Cossi, G. Scalmani, N. Rega, G. A. Petersson, H. Nakatsuji, M. Hada, M. Ehara, K. Toyota, R. Fukuda, J. Hasegawa, M. Ishida, T. Nakajima, Y. Honda, O. Kitao, H. akai, M. L. Klene, X., J. E. Knox, H. P. Hratchian, J. B. Cross, V. Bakken, C. Adamo, J. Jaramillo, R. Gomperts, R. E. Stratmann, O. Yazyev, A. J. Austin, R. Cammi, C. Pomelli, J. W. Ochterski, P. Y. Ayala, K. Morokuma, G. A. Voth, P. Salvador, J. J. Dannenberg, V. G. Zakrzewski, S. Dapprich, A. D. Daniels, M. C. Strain, O. Farkas, D. K. Malick, A. D. Rabuck, K. Raghavachari, J. B. Foresman, J. V. Ortiz, Q. Cui, A. G. Baboul, S. Clifford, J. Cioslowski, B. B. Stefanov, G. Liu, A. Liashenko, P. Piskorz, I. Komaromi, R. L. Martin, D. J. Fox, T. Keith, M. A. Al-Laham, C. Y. Peng, A. Nanayakkara, M. Challacombe, P. M. W. Gill, B. Johnson, W. Chen, M. W. Wong, C. Gonzalez, J. A. Pople, Gaussian, Inc., Wallingford CT, **2004**.
14. Martin Gouterman. The porphyrins. Academic Press. Inc., 1978.
15. Dage Sundholm, *Phys. Chem. Chem. Phys.*, **2000**, 2, 2275-2281.
16. Sreedharan Prathapan, Sung Ik Yang, Jyoti Seth, Mark A. Miller, David F. Bocian, Dewey Holten, and Jonathan S. Lindsey, *J. Phys. Chem. B*, **2001**, *105* (34), 8237–8248.

6. Acknowledgements

Financial support by the MRG-WII colabbolation with Chulalongkorn university project 515S045 , RTA project 4980006 given in the frame of the Thailand research fund and National center of excellence for petroleum, petrochemicals, and advanced materials (NCE-PPAM). All facilities and computer resources are provided by the Computational Chemistry Unit Cell at Department of Chemistry, Faculty of Science, Chulalongkorn University.

VITAE

NAME: Tatiya Chokbunpiam

DATE AND PLACE OF BIRTH: 3 April 1984 in Bangkok, Thailand

ELEMENTARY SCHOOL:

1991-1997	Sriwittayapaknam School, Samutprakan

SECONDARY SCHOOL:

1997-2003	Samutprakan School, Samutprakan

EDUCATION:

2003-2007	B. Sc. in General Science, Department of Chemistry, Faculty of Liberal Arts and Science, Kasetsart University, Kamphaeng Saen Campus
2007-2009	M. Sc. in Petrochemistry and Polymer Science, Faculty of Science, Chulalongkorn University, Bangkok

AWARDS:

2009	The outstanding poster presentation award the pure and applied chemistry international conference
2009	The outstanding paper in computational chemistry session international annual symposium on computational science and engineering